13 Theoretical Analysis of Shear Localization in the Lithosphere

David Bercovici and Shun-ichiro Karato

Department of Geology and Geophysics
Yale University
New Haven, Connecticut 06511

INTRODUCTION

Deformation in the Earth is rarely homogeneous and often occurs in narrow regions of concentrated strain referred to as zones of shear localization. Mylonites found in the continental crust are the manifestation of shear localization (White et al. 1980) and, at the largest scale, shear localization is proposed to be crucial for the generation of tectonic plates from a convecting mantle (Bercovici 1993, 1995b,a, 1996, 1998; Bercovici et al. 2000; Trompert and Hansen 1998; Tackley 1998, 2000a,b,c,d). Shear localization is apparent in many field of physics, including, for example, metallurgy (Lemonds and Needleman 1986), rock mechanics (Poirier 1980; Jin et al. 1998), granular dynamics (Scott 1996; Géminard et al. 1999, e.g.) and glaciology (Yuen and Schubert 1979). However, basic solid-state rheologies, such as elasticity, visco-elasticity, viscous flow and even steady-state non-Newtonian viscous flow, are insufficient by themselves to generate shear-localization; this is because in all such rheologies an increase in deformation or rate of deformation results in greater resistance (i.e., stress) instead of self-weakening and loss of strength. Shear-localization tends to require dynamic feedback mechanisms wherein self-weakening is controlled by a macroscopic variable (such as temperature) or microscopic structure (grain size or microcrack density) whose evolution and concentration are themselves determined by deformation; in this way deformation can induce weakening, which subsequently causes deformation to concentrate on the weak zone (being most easily deformed), causing further weakening, and thus more focusing of deformation, and so on.

One of the most fundamental manifestations of such feedback mechanisms arises from the coupling of viscous heating and temperature-dependent viscosity wherein the zone of dissipative heating weakens and thus focuses deformation, leading to further heating and weakening; this mechanism is thought applicable to problems in metal weakening, glacial surges, and lithosphere dynamics (Schubert and Turcotte 1972; Yuen and Schubert 1979; Poirier 1980; Balachandar et al. 1995; Bercovici 1996; Thatcher and England 1998). In granular media, localization is due to dilation of the medium leading to effectively weaker rarifed zones that concentrate deformation, which in turn agitates the medium causing further dilation (Géminard et al. 1999); this phenomenon is of potential importance in earthquake dynamics (Scott 1996; Marone 1998; Segall and Rice 1995; Sleep 1995, 1997; Mora and Place 1998). Another shear localization mechanism arises from the reduction of grain size under stress in solid-state creep mechanisms which have grainsize-dependent viscosities (i.e., grain reduction leads to zones of weakness which concentrate deformation, increasing stress and thus further reducing grain size and enhancing weakening); this mechanism has been proposed to be the cause for mylonitic shear zones and is thought to be a basic ingredient of crustal and lithospheric deformation (Kameyama et al. 1997; Jin et al. 1998; Braun et al. 1999). Finally, material that undergoes brittle or combined brittle-ductile

1529-6466/00/0051-0013$05.00

deformation can, with large strain, experience concentration of microcrack and void populations developing weak bands on which deformation focuses, leading to further cracking, weakening, and invariably shear localization. This phenomenon occurs in the process of dilatant plasticity in metals as well as crustal rocks (Lemonds and Needleman 1986; Ashby and Sammis 1990; Lemaitre 1992; Hansen and Schreyer 1992; Lockner 1995; Mathur et al. 1996; Krajcinovic 1996; Lyakhovsky et al. 1997; Regenauer-Lieb 1999). The inference that much of the lithosphere undergoes combined brittle-ductile behavior (Kohlstedt et al. 1995; Evans and Kohlstedt 1995), combined with the longevity of plate boundaries (Gurnis et al. 2000), have motivated some (Bercovici 1998; Tackley 1998; Bercovici et al. 2001a,b; Bercovici and Ricard 2003; Auth et al. 2002) to consider that the primary weakening mechanism that leads to plate boundary formation is due to damage, that is, semi-ductile void and microcrack formation.

In this paper we examine in some mathematical detail the fundamental physics of shear-localizing feedback mechanisms by using the basic model of a simple-shear layer. Such a layer could represent anything from a strike-slip shear zone to a subducting slab to a glacial gravity flow, etc. Simple one-dimensional shear-flows have been considered many times before, primarily for viscous-heating and thermal-runaway effects (e.g., Yuen and Schubert 1977; Schubert and Yuen 1978; Fleitout and Froidevaux 1980). Here, we will use this model to examine three basic feedback mechanisms thought relevant to the mantle and lithosphere, i.e., (1) viscous heating with temperature-dependent viscosity; (2) a simple damage formulation to model semiductile-semibrittle behavior; and (3) grainsize-dependent rheology and recrystallization. (While we focus on only three basic mechanisms, a more complete survey of many shear-localizing mechanisms, but with less mathematical detail, is provided by Regenauer-Lieb and Yuen (2002).) An important aspect of any feedback mechanism is not only how a rheology-controlling macroscopic or microscopic property is enhanced by deformation, but also how that property is restored, lost, equilibrated or "healed"; thus we will also consider some basic healing mechanisms. After our foray into simply theory, we will discuss recent progress on some of the more complicated aspects of these feedback mechanisms, and will close with a brief summary.

THEORETICAL PRELIMINARIES

To illustrate the essential physics of shear localization with various rheological mechanisms, we consider a model of unidirectional simple-shear flow in an infinitely long channel. The channel is infinite in the x and z directions and is $2L$ wide, with boundaries at $y = \pm L$ that move in opposite directions along the x direction. Since the channel is uniform and infinite in x and z, none of the properties of the medium (stress, velocity, temperature, etc.) are functions of x and z, but only of y and time t. In this case, the general force balance equation (i.e., assuming slow creeping flow and thus negligible acceleration terms) is

$$0 = -\boldsymbol{\nabla} P + \boldsymbol{\nabla} \cdot \underline{\boldsymbol{\sigma}} + \rho \boldsymbol{g} \tag{1}$$

where P is pressure or isotropic stress, $\underline{\boldsymbol{\sigma}}$ the deviatoric stress tensor, ρ the density and $\boldsymbol{g}$ the gravitational acceleration vector. The component of this equation in the x direction, given that there is no dependence on x and z (assuming that $\boldsymbol{g}$ is only in the z direction)

becomes

$$0 = \frac{\partial \sigma_{yx}}{\partial y} \tag{2}$$

where σ_{yx} is the shear stress that is acting on surfaces facing in the y direction but pulling on them in the x direction. The above equation implies that $\sigma_{yx} = \sigma$ which is a constant in y.

For viscous flows, shear localization is measured in terms of strain-rate,

$$\underline{\dot{\boldsymbol{\varepsilon}}} = \tfrac{1}{2}(\boldsymbol{\nabla v} + [\boldsymbol{\nabla v}]^t) \tag{3}$$

where $\underline{\dot{\boldsymbol{\varepsilon}}}$ is the strain-rate tensor and $\boldsymbol{v}$ the velocity vector. In our example $\boldsymbol{v} = u(y)\hat{\boldsymbol{x}}$ where u is the velocity in the x direction and $\hat{\boldsymbol{x}}$ the unit vector in the x direction; thus the strain-rate tensor has only one unique component $\dot{\varepsilon}_{yx} = \frac{1}{2}\frac{\partial u}{\partial y}$.

We make the simplifying assumption that stress is related to strain-rate plus only one other variable which we'll denote for now by Θ which is either temperature, void fraction or grainsize. The constitutive relation between stress and strain rate is thus

$$\underline{\boldsymbol{\sigma}} = 2\mu(\Theta, \dot{\varepsilon})\underline{\dot{\boldsymbol{\varepsilon}}} + \eta \boldsymbol{\nabla} \cdot \boldsymbol{v}\underline{\boldsymbol{I}} \tag{4}$$

where μ is viscosity, $\dot{\varepsilon}^2 = \frac{1}{2}\underline{\dot{\boldsymbol{\varepsilon}}} : \underline{\dot{\boldsymbol{\varepsilon}}}$ (which is related to the 2nd strain-rate invariant), and η is a material property which includes the bulk viscosity. In our example, since $\boldsymbol{v} = u(y)\hat{\boldsymbol{x}}$ there is ony one stress and one strain-rate and our constitutive law becomes

$$\sigma = 2\mu(\Theta, \dot{\varepsilon})\dot{\varepsilon} \tag{5}$$

where $\dot{\varepsilon} = \frac{1}{2}\frac{\partial u}{\partial y}$.

If the relation between stress and strain-rate is monotonic (i.e., an increase in one always causes an increase in the other), and there is no feedback between strain-rate and the state variable Θ, then there can be no localization in our example. In particular, say we employ a power-law rheology, then $\mu = \frac{1}{2}A\dot{\varepsilon}^{\frac{1-n}{n}}$ where A is a constant and n is the power-law index. For pseudo-plastics (like many food products such as mustard and ketchup, and silicates in the dislocation-creep regime) $n > 1$ so that viscosity decreases with increasing strain-rate. However, stress and thus resistance to motion, or strength, $\sigma = A\dot{\varepsilon}^{1/n}$ always increases with strain-rate, even if the viscosity decreases. Moreover, in our example, $\dot{\varepsilon} = (\sigma/A)^n$ is a constant across the layer because σ and A are constants, and thus without any heterogeneity in strain-rate, there is no shear-localization anywhere in the layer.

For the model system to develop shear-localization, it must allow non-constant strain-rate across the layer (the localization is a region of high strain-rate surrounded by low-strain rate). This can be accomplished in our model if the effective stress–strain-rate relation is non-monotonic (i.e., there is a maximum or minimum stress), such that one stress can yield at least two-possible strain-rates. As we show below, such an effective rheology generally arises from a feedback between the state variable Θ and the stress or strain-rate.

SHEAR LOCALIZING FEEDBACK MECHANISMS

One requirement of a feedback mechanism that permits shear-localization is that the evolution of Θ must depend on the deformation, i.e., strain or strain-rate of the system; in

our examples we will focus on completely irrecoverable deformation and thus work with strain-rate (i.e., we will take a viscous-flow approach). Thus, for a feedback mechanism to exist, an increase in strain-rate must lead to a change in Θ that subsequently reduces the viscosity, causing (through Eqn. 5) yet larger strain-rate, and so on. We will examine our three basic feedback mechanisms (thermal, simple-damage and grainsize controlled) for simple decay-type loss mechanisms that facilitate the analysis. The decay-loss mechanism, however, is not always realistic in the case of thermally-controlled, and possibly even damage-controlled feedback mechanisms, wherein diffusive loss is as important; therefore, we will analyze these feedbacks for diffusive loss as well, which leads to different mathematical solutions but the interpretation is related to the simpler decay-loss cases.

Thermal feedback with decay-loss healing

In considering the feedback between viscous heating and temperature-dependent viscosity, we define Θ to be temperature T. The evolution equation for T involving temporal change, advective transport, decay loss and a deformation-related source term is

$$\rho c_p \left(\frac{\partial T}{\partial t} + \boldsymbol{v} \cdot \boldsymbol{\nabla} T \right) = -K(T - T_0) + 2\mu(T, \dot{\varepsilon})\dot{\varepsilon}^2 \tag{6}$$

where ρ is density, c_p is heat capacity, K is a heat-transfer coefficient, and T_0 is the value of T to which the unforced system equilibrates (e.g., it could be the temperature of heat reservoirs in contact with the boundaries of the channel). A heat-transfer coefficient can be used instead of diffusive loss if the layer thickness L is very small (in which case $K \sim k/L^2$ where k is thermal conductivity). The last term on the right represents the deformational work, which for simple single-phase systems goes into dissipative heating and thus an increase in internal/thermal energy (i.e., via an increase in entropy). As discussed in the next subsection, in multi-phase systems, part of this work can also go into creation of surface energy by, say, creating new microcracks, voids and/or defects.

Given the nature of our simple one-dimensional system, Equation (6) becomes

$$\rho c_p \frac{\partial T}{\partial t} = -K(T - T_0) + 2\mu(T, \dot{\varepsilon})\dot{\varepsilon}^2 \tag{7}$$

Let us first consider steady-state solutions such that Equation (7) becomes

$$K(T - T_0) = 2\mu(T, \dot{\varepsilon})\dot{\varepsilon}^2 \tag{8}$$

To solve this system we must specify the viscosity law for $\mu(T, \dot{\varepsilon})$. Materials that undergo solid-state creep (diffusion or dislocation creep) have a temperature-dependence of viscosity given by an Arrhenius factor; for our 1-D system the viscosity law can be written in as

$$\mu = \tfrac{1}{2} A e^{\frac{H}{nRT}} \dot{\varepsilon}^{\frac{1-n}{n}} \tag{9}$$

where A is constant, H is the activation enthalpy, R the gas constant and n the power-law index; for Newtonian diffusion creep $n = 1$, while typical values for non-Newtonian dislocation creep in rocks is $n = 3$ to 5. We can reduce the number of free parameters by defining variables in terms of the natural scales of the system. We define $T = T_0 + T^*\theta$ and $\dot{\varepsilon} = \dot{\varepsilon}^*\dot{\varepsilon}'$ where T^* and $\dot{\varepsilon}^*$ are as-yet-unknown scales, and θ and $\dot{\varepsilon}'$ are dimensionless

temperature and strain-rate, respectively. Substituting these expressions into Equation (8) while using Equation (9) leads to (dropping primes for simplicity)

$$\left[\frac{KT^*}{A(\dot{\varepsilon}^*)^{\frac{1+n}{n}}}\right]\theta = e^{\left[\frac{H}{RT^*}\right]\frac{1}{n(\theta_0+\theta)}}\dot{\varepsilon}^{\frac{1+n}{n}} \tag{10}$$

where $\theta_0 = T_0/T^*$. Likewise, the constitutive law Equation (5)–along with Equation (9)–becomes

$$\left[\frac{\sigma}{A(\dot{\varepsilon}^*)^{1/n}}\right] = e^{\left[\frac{H}{RT^*}\right]\frac{1}{n(\theta_0+\theta)}}\dot{\varepsilon}^{\frac{1}{n}} \tag{11}$$

The expressions in square brackets are dimensionless groups, and we can choose T^* and $\dot{\varepsilon}^*$ to make two of these go to unity. In particular, we define

$$T^* = \frac{H}{R} \text{ and } \dot{\varepsilon}^* = \left(\frac{KH}{RA}\right)^{\frac{n}{n+1}} \tag{12}$$

such that Equation (10) and Equation (11) become our steady-state governing equations:

$$\theta = \left(e^{\frac{1}{\theta_0+\theta}}\dot{\varepsilon}^{n+1}\right)^{\frac{1}{n}} \tag{13}$$

and

$$\tau = \left(e^{\frac{1}{\theta_0+\theta}}\dot{\varepsilon}\right)^{\frac{1}{n}} \tag{14}$$

respectively, where

$$\tau = \sigma\left(\frac{R}{A^n KH}\right)^{\frac{1}{n+1}} \tag{15}$$

Although we have reduced the number of free parameters, our system still depends on the dimensionless boundary or background temperature θ_0 and the power-law index n. Note that since we have chosen $H/R \approx 6\times10^4$ K as our temperature scale (i.e., $H \approx 500$ kJ/mol and and $R \approx 8$ J/K/mol), then our typical backround lithospheric nondimensional temperature θ_0 will be of order 10^{-2}. We will, however, also examine higher background temperatures for the sake of comparison.

Equation (13) and Equation (14) lead to a parametric equation for stress and strain-rate (i.e., τ and $\dot{\varepsilon}$ are functions of each other through the "parameter" θ)

$$\tau = \left(\theta e^{\frac{1}{\theta_0+\theta}}\right)^{\frac{1}{n+1}} \quad , \quad \dot{\varepsilon} = \left(\theta^n e^{-\frac{1}{\theta_0+\theta}}\right)^{\frac{1}{n+1}} \tag{16}$$

which is thus an effective constitutive law. Curves for the effective constitutive relations for τ versus $\dot{\varepsilon}$ for various n and θ_0 are shown in Figure **1**. In this case a variety of behavior is available. For large θ_0 one can obtain a simple power-law like behavior wherein stress monotonically increases with strain-rate and thus no shear-localization is possible. For relatively low θ_0 a non-monotonic effective stress–strain-rate constitutive relation occurs which therefore permits multiple strain-rates across the layer and the possibility of shear

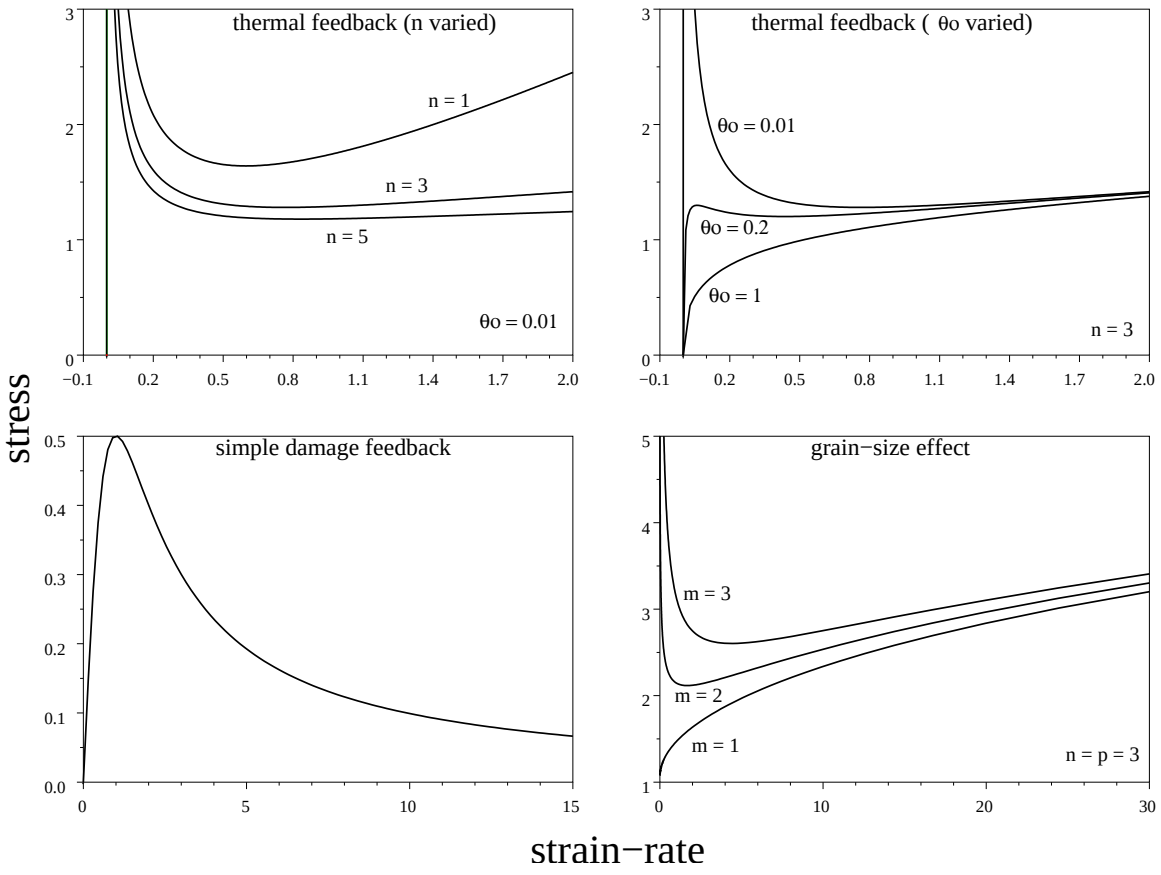

Figure 1: Effective "stress versus strain-rate" constitutive laws for three different feedback mechanisms with decay-type loss, as discussed in the text. The top two panels show the thermal feedback, i.e., where the sheared layer undergoes viscous heating that then influences the viscosity because of its temperature dependence. In these cases viscosity is possibly also a function of strain-rate through a power-law dependence that is controlled by the power-law index n (i.e., if $n = 1$ there is no dependence on strain-rate, and for $n > 1$ viscosity decreases with increasing strain-rate). The top left panel considers the thermal feedback with the background or boundary temperature θ_0 fixed at the value indicated, and for three different power-law indices n. The top right panel shows the same feedback for different background temperatures and one power-law index. For low enough background temperatures there is a region at low strain-rates where stress rapidly increases and then decreases with increasing strain-rate, which implies a resistance build-up and strength loss akin to stick-slip behavior. For yet higher strain-rates stress begins to increase again indicating a strength recovery; however, the rate of recovery with increasing strain-rate is much less for larger power-law indices n. For high background temperatures, there is no stick-slip-type region. The bottom two panels show feedback mechanisms for simple damage (deformation increases void/microcrack density which in turn reduces viscosity) and grainsize effects (stress reduces grain size which reduces viscosity). The damage mechanism gives a very simple stick-slip-type behavior with no strength-recovery. The grainsize effect is dependent on power-law index n, and indices that control the grainsize dependence of viscosity m (if $m = 0$ viscosity is grainsize independent) and the grainsize dependence of grain growth p (if $p = 1$ grain-growth is grainsize independent). Stick-slip behavior in the grainsize feedback mechanism occurs with no finite resistance build-up; i.e., resistance is effectively infinite when strain-rate is infinitesimally small. For increasing strain-rate there is strength loss and recovery also. However, the stick-slip type behavior only exists for sufficient grainsize dependence of viscosity, i.e., $m > 1$.

localization. Indeed, in these low-θ_0 cases, as many as three possible strain-rates can occur for a given stress (i.e., the constitutive curves have both a local maximum and a minimum).

The constitutive curves that involve multiple strain-rates for a given stress are also considered to have a pseudo-stick-slip behavior. In particular, at low strain-rates the material resistance is large and climbs rapidly with increased deformation-rate, what would be analogous to "stick" behavior. At a peak stress, however, stress and resistance give way to the "slip" behavior and loss of resistance or strength with increased strain-rate (the region of the constitutive curve with negative slope). In the thermal feedback, stress eventually begins to climb again at high strain-rates, albeit very gradually, as is characteristic of deformation in a hot, low-viscosity medium (which of course, at these high strain-rates and dissipative heating, it is). Such strength loss and stick-slip behavior is often considered closely associated with shear-localization.

The multiplicity of states (which then leads to mulitple strain-rates) in this system is illustrated by considering the possible solutions to temperature θ in the steady-state system; these are of course the roots to Equation (13) and Equation (14), which can be combined into one transcendental equation

$$\theta e^{\frac{1}{\theta_0+\theta}} = \tau^{n+1} \tag{17}$$

These roots as functions of stress τ are shown in Figure **2**. Three roots are possible, and these represent a cold, highly viscous one (near $\theta = 0$), an intermediate-temperature one and a hot, low-viscosity one.

There are, however, several constraints on the existence of these three roots. For a background temperature $\theta_0 < 1/4$, the function $\theta e^{\frac{1}{\theta_0+\theta}}$ has two local extrema (a local maximum and minimum), and for $\theta_0 > 1/4$ it has no local extrema (only a monotonic increase with θ). Thus, for $\theta_0 < 1/4$ there are three possible solutions to Equation (17), but for larger θ_0 there is only one solution. Nevertheless, the temperature scale H/R is so large that essentially all realistic lithospheric temperatures will satisfy the constraint of $\theta_0 < 1/4$.

There is a further constraint on the possibility of shear localization in that the three possible roots only exist for τ^{n+1} beneath a maximum, as shown in Figure **2**, which is itself a function of θ_0. For plausible lithospheric values of $\theta_0 \sim O(10^{-2})$, the maximum stress is given by $\tau^{n+1} \approx 10^{38}$ (see Fig. **2**). The scale factor by which we redimensionalize τ is given by Equation (15); we can estimate this factor using typical silicate values for the given constants, namely $n = 3$, $A^n = 2.5 \times 10^{-6}$ MPa^3 s, (e.g., see Turcotte and Schubert 1982), $H/R \approx 6 \times 10^4$ K (see above), and $K = k/L^2 \approx 4 \times 10^{-14}$ MPa K^{-1} s^{-1} assuming $L \leq 10$ km. With the resulting scale factor, which is of the order 10^{-4} MPa, and the critical value of $\tau \approx 3 \times 10^9$ (having used $n = 3$) we find the maximum σ is of the order of 10^6 MPa. Thus essentially all tectonic stresses will fall below this maximum stress and thus permit multiple solutions and thus shear localization.

However, because steady-state solutions to these equations exist does not mean they are stable against perturbations. Although we could perform a linear stability analysis of these solutions, or even calculate a full nonlinear time-dependent solution, it is instructive to inspect the evolution equation. In particular, if we nondimensionalize time by $\rho c_p/K$, then

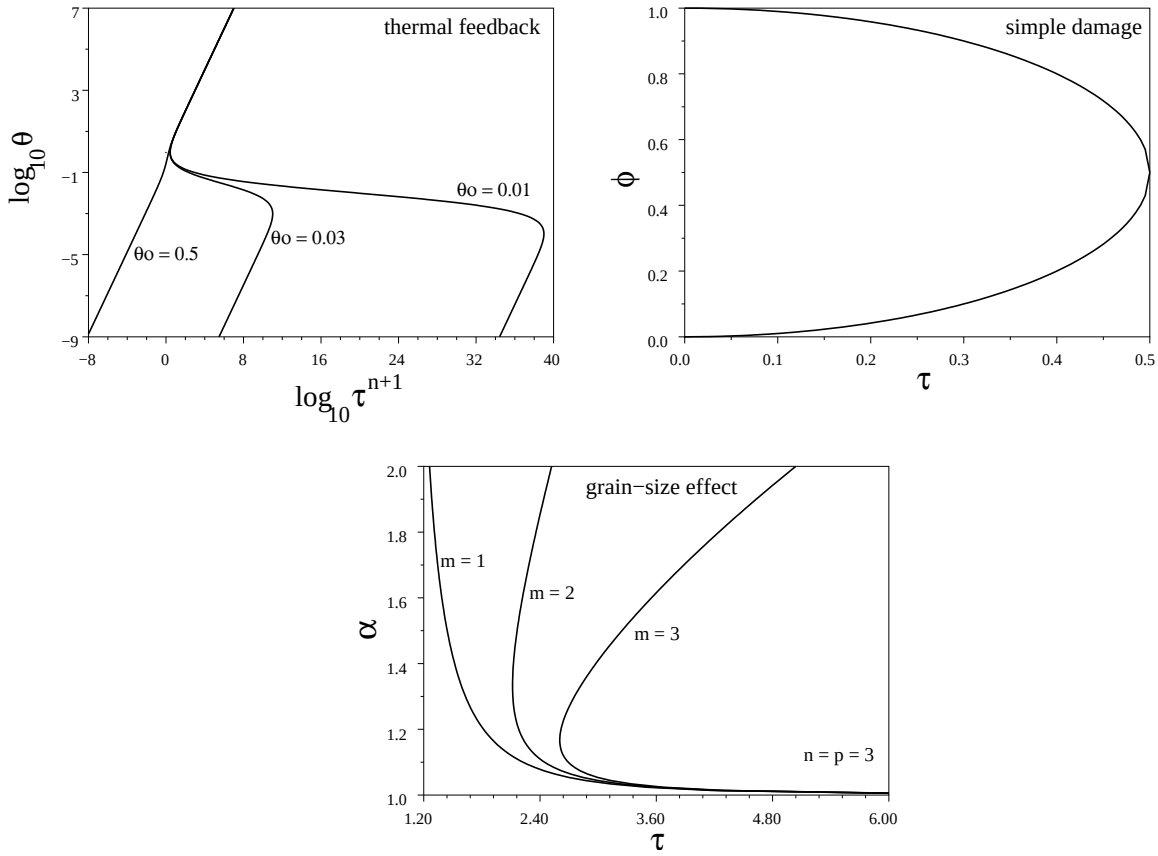

Figure 2: Solutions of the state variables (temperature θ, void density ϕ and grainsize α) as functions of stress τ for the same three feedback mechanisms of Figure **1**. For each mechanism at least two possible solutions exist for a single stress τ. Since multiple possible states exist for one stress across the sheared layer, then mulitple viscosities and strain-rates can exist within the layer also, which is a condition for shear-localization (since it implies nonhomogenous shear). For the thermal feedback mechanism, three possible solutions exist for stresses beneath a maximum τ which is itself a function of background temperature θ_0 and power-law index n (note n is absorbed into the abscissa of the plot). The damage mechanism allows two possible solutions for a given stress beneath a maximum stress $\tau = 1/2$. For the grainsize mechanism, however, two possible solutions exist if the grainsize dependent of viscosity is sufficient (i.e., $m > 1$) and such multiple solutions exist only for a stress above a minimum value, instead of beneath a maximum as with the other two feedback mechanisms.

along with the other nondimensionalization steps discussed above, Equation (7) becomes

$$\frac{\partial \theta}{\partial t} = -\theta + \tau^{n+1} e^{-\frac{1}{\theta_0 + \theta}} \tag{18}$$

If we plot $\frac{\partial \theta}{\partial t}$ versus θ (Fig. **3**) – a plot often referred to in dynamical systems as a phase diagram– we can see that the steady solutions occur where the curves intersect the $\frac{\partial \theta}{\partial t} = 0$ line. The stability of either steady solution is given by the the slope of the curve at the relevant interesection. If the slope is negative at the steady solution then it is stable; i.e., solutions on the curve to either side of the steady one will evolve to the steady solution (in particular, if the solution is to the left of the steady case with a smaller θ then its growth rate is positive and it will grow toward the steady value; if it is to the right with a larger θ, the growth rate is negative and the solution will decay to the steady value). In contrast if

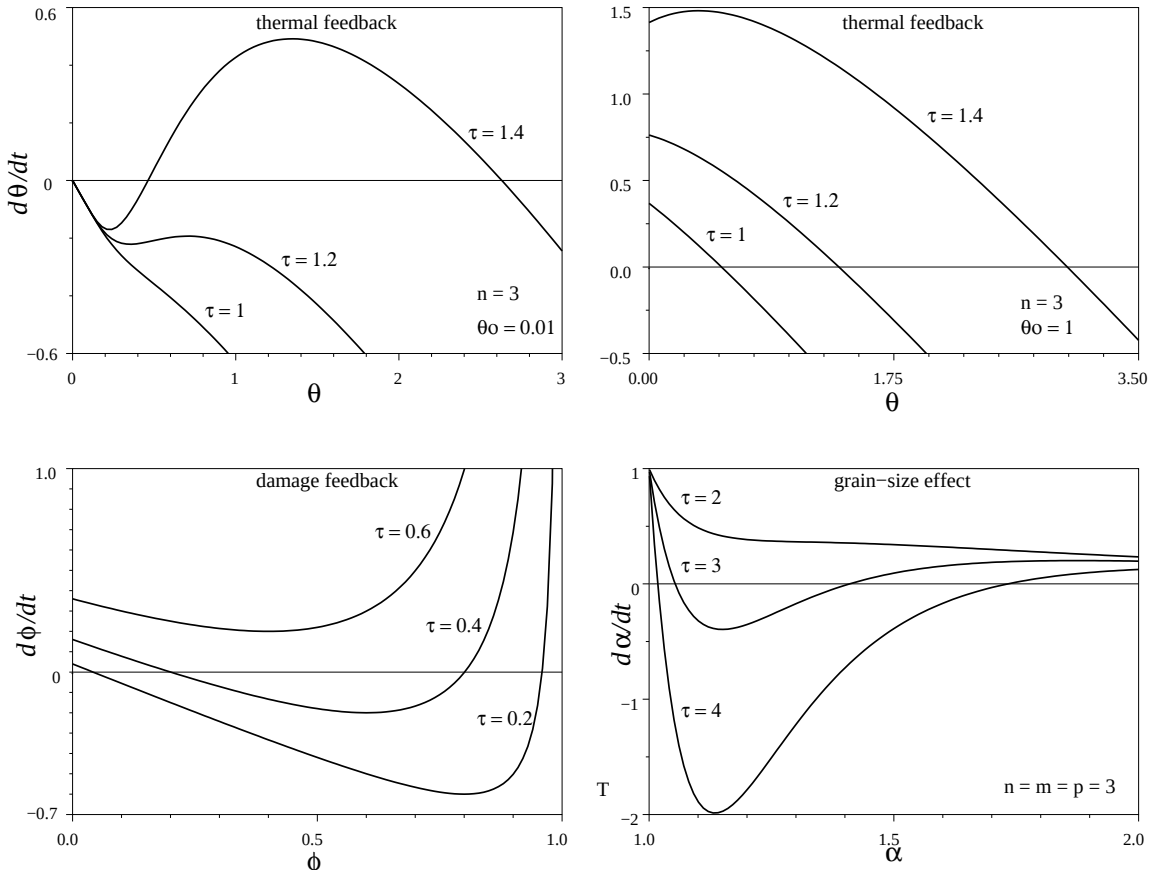

Figure 3: Phase diagrams for the same three feedback mechanisms of Figures **1** and **2**, which show time-rate of change of the state variables versus the state variables themselves (i.e., temperature θ, void density ϕ and grainsize α). All panels show phase trajectories for different values of stress τ as indicated; the top two panels show the thermal feedback with two different background temperatures θ_0. These phase diagrams illustrate the temporal behavior of the feedback mechanisms and the stability of the steady solutions illustrated in Figure **2**. Steady solutions occur where the phase trajectory crosses the line where the time-rate of change is zero. The trajectory slope at these intersections indicates the stability of the steady solution; i.e., the solution is unstable if the slope is positive, and stable if negative (see text for further discussion). Trajectories that do not cross the zero-rate line have no steady solution. See text for further discussion.

the slope is positive at the steady solution then that solution is unstable (solutions to either side of the steady one will diverge from it). In the case of Equation (18) (Fig. **3**) we see that if the background temperature θ_0 is sufficiently small (such that there are three possible steady solutions) then both the cold/viscous and the hot/low-viscosity cases are stable ($d\theta/dt$ vs. θ has a negative slope at that root), while the intermediate-temperature case is unstable. Therefore unsteady solutions in the vicinity of the intermediate-temperature root will evolve toward one or the other stable root; temperatures hotter than the intermediate case will grow to the hot steady state, and colder temperatures will go to the cold case. Therefore, since the layer will in the end have two different temperatures and two strain-rates, then weak zones and localization can be expected to occur (as long as the initial temperature is in the vicinity of the intermediate root). However, when a localized weak zone develops, it cannot weaken and localize without bound but must stop at the hot/low-viscosity solution. Thus a fault-like shear localization is impossible for this mechanism. However, it should be noted that given the temperature scale $H/R \approx 6 \times 10^4$ K both the

intermediate and hot/low-viscosity roots are at temperatures near or well in excess of the melting temperature. Therefore, this mechanism would in fact give way to a melting instability well before these roots were reached. With such melting and extreme viscosity and strength drop, an extremely sharp localization is possible, although that is beyond the simple physics we are exploring in this model.

Simple-damage feedback with decay-loss healing

The large region of the lithosphere that is thought to undergo combined brittle-ductile behavior (Kohlstedt et al. 1995) is suggestive of a damage-induced shear localization whereby microcracks forming in zones of ductile deformation focus into weak zones that thereby concentrate deformation and accelerate their own nucleation and growth, in the end creating distinct shear bands that appear like faults. Damage-induced shear localization is also appealing given the various roles it offers for water, which is thought to be a facilitator of plate tectonics, and the cause for plate tectonics on Earth but not the other terrestrial planets (Tozer 1985). For example, volatiles such as water can either facilitate damage through hydro-fracturing, pore-pressure-reduction of friction and simple lubrication of slip zones; and/or the damaged material (with finite pore space and open grain boundaries) can facilitate hydrolytic weakening of minerals and/or pressure-solution creep (Guéguen and Palciauskas 1994; Ranalli 1995). Although the role of water has generally been thought to be confined to only the upper few tens of kilometers of the lithosphere, there is growing evidence that it is present and influencing Earth's rheology and evolution at hundreds of kilometers depth (Hirth and Kohlstedt 1996; Karato 2002).

A simplified viscous damage theory termed the "void-volatile" mechanism (Bercovici, 1998; see also Regenauer-Lieb, 1999) involves modelling the evolution of microcrack or void density with a scalar transport law in which deformational work provides the source for void creation (similar to the heat-transport equation with frictional heating included). In this case, the weakening variable Θ is set equivalent to void volume fraction (i.e., porosity) Φ, and we write a simple transport law which in our 1-D example is

$$\rho c \frac{\partial \Phi}{\partial t} = -B(\Phi - \Phi_0) + 2f\mu(\Phi, \dot{\varepsilon})\dot{\varepsilon}^2 \tag{19}$$

where c is the proportionality factor between Φ and energy per unit mass, B is analogous to K, and Φ_0 is the background value of Φ to which the unforced system equilibrates. In this equation we have assumed that some fraction f of the deformational work goes into creation of surface energy by creating new microcracks, voids and/or defects; this is often referred to as stored-work, or, as discussed in the 1920s by G.I. Taylor, through his experiments on torsional deformation of metals, as latent-heat of cold work (Farren and Taylor 1925; Taylor and Quinney 1934). Finally, we assume a linear dependence of viscosity on Φ, which is relevant for the sort of two-phase mixtures assumed here (Bercovici 1998; Ricard et al. 2001). In particular, if the mixture is of a solid matrix with viscosity μ_m and a void-filling fluid with viscosity μ_f, then simple mixture theory will yield an effective viscosity of $\mu_f\Phi + \mu_m(1-\Phi)$, which can be recast as

$$\mu = \mu_r(1 - \lambda\Phi) \tag{20}$$

where $\mu_r = \mu_m$ is the reference viscosity and $\lambda = (\mu_m - \mu_f)/\mu_m$ controls viscosity variability.

Again we first consider steady solutions to Equation (19), i.e., solutions of

$$B(\Phi - \Phi_0) = 2f\mu_r(1 - \lambda\Phi)\dot{\varepsilon}^2 \tag{21}$$

To reduce the number of free parameters in the system, we again use the natural scales of the system by first defining

$$\Phi = \Phi_0 + \Phi^*\phi \tag{22}$$

where Φ^* is an as yet unknown porosity scale and ϕ is a rescaled porosity perturbation. In this case we rewrite viscosity as

$$\mu = \mu_0\left(1 - \frac{\lambda\Phi^*}{1 - \lambda\Phi_0}\phi\right) \tag{23}$$

where $\mu_0 = \mu_r(1 - \lambda\Phi_0)$. At this point we can define the porosity scale as

$$\Phi^* = (1 - \lambda\Phi_0)/\lambda \tag{24}$$

such that our viscosity law becomes

$$\mu = \mu_0(1 - \phi) \tag{25}$$

We define strain-rate also in terms of a dimensionless quantity, namely $\dot{\varepsilon} = \dot{\varepsilon}^*\dot{\varepsilon}'$ where $\dot{\varepsilon}^*$ is a dimensional scale and $\dot{\varepsilon}'$ is a dimensionless variable. In this case, the constitutive law (Eqn. 5 using $\Theta = \Phi$) leads to

$$\left[\frac{\sigma}{2\mu_0\dot{\varepsilon}^*}\right] = (1 - \phi)\dot{\varepsilon}' \tag{26}$$

and Equation (21) becomes

$$\left[\frac{B(1 - \lambda\Phi_0)}{2f\lambda\mu_0(\dot{\varepsilon}^*)^2}\right]\phi = (1 - \phi)\dot{\varepsilon}'^2 \tag{27}$$

where the terms in square brackets are dimensionless groups. We choose our strain-rate scale to set one of these groups to unity:

$$\dot{\varepsilon}^* = \sqrt{\frac{B(1 - \lambda\Phi_0)}{2f\lambda\mu_0}} = \sqrt{\frac{B}{2f\lambda\mu_r}} \tag{28}$$

Thus, our two governing equations, Equation (26) and Equation (27) become, after dropping the primes,

$$\tau = (1 - \phi)\dot{\varepsilon} \tag{29}$$

and

$$\phi = (1 - \phi)\dot{\varepsilon}^2 \tag{30}$$

where

$$\tau = \sigma\sqrt{\frac{f\lambda}{2\mu_0 B(1 - \lambda\Phi_0)}} \tag{31}$$

represents a dimensionless imposed stress. With these equations we can eliminate ϕ to arrive at an effective constitutive law

$$\tau = \frac{\dot{\varepsilon}}{1+\dot{\varepsilon}^2} \tag{32}$$

which is shown in Figure **1**. As noted in the previous section, because stress increases sharply below a certain strain-rate (in this case at $\dot{\varepsilon} < 1$) and then decreases for higher strain-rates, this effective constitutive law has been referred to explicitly as a stick-slip rheology (Whitehead and Gans 1974; Bercovici 1993). However, in contrast to the thermal feedback mechanism, the material continues to lose strength (stress decreases) as strain-rate goes to infinity; this implies that effectively infinite strain rates can be achieved, and the ongoing strength loss is indicative of a runaway effect, which will become more evident momentarily.

Apart from the effective constitutive law, the actual solutions for ϕ and $\dot{\varepsilon}$ in terms of τ are instructive for inferring shear-localization in the layer. The steady-state solutions require

$$\phi = \tfrac{1}{2}(1 \pm \sqrt{1-4\tau^2}) \quad \text{and} \quad \dot{\varepsilon} = \frac{1}{2\tau}(1 \pm \sqrt{1-4\tau^2}) \tag{33}$$

and thus for a given τ there are two possible porosities and strain-rates, a high-porosity/fast (i.e., rapidly deforming) one associated with the $+$ root, and a low-porosity/slow case associated with the $-$ root (Fig. **2**). Shear localization requires inhomogeneous strain-rate, i.e., for a given stress across the layer localization requires at least two possible strain-rates to co-exist, which this feedback mechanism also provides. Again, shear localization would be manifest if the layer contained some regions with the slow solution and some with the fast solution (the localizations would then be the fast zones).

Equation (33) shows that there are no steady-state solutions if $\tau > \frac{1}{2}$, in which case there are only time-dependent solutions. We can infer both the nature of time-dependent solutions and the stability of steady-state solutions by inspecting the evolution equation Equation (19). In particular, if we nondimensionalize time by $\rho c/B$, then along with the other nondimensionalization steps discussed above, Equation (19) becomes

$$\frac{\partial \phi}{\partial t} = -\phi + \frac{\tau^2}{1-\phi} \tag{34}$$

If we plot $\frac{\partial \phi}{\partial t}$ versus ϕ (Fig. **3**) we again see that the steady solutions occur where the curves intersect the $\frac{\partial \phi}{\partial t} = 0$ line and the stability of steady solutions is given by the the slope of the curve at the relevant interesection. In this case, the low-porosity/slow steady solution is stable and the high-porosity/fast one is unstable. However, this does not mean that the system will everywhere evolve to the slow solution; indeed, values of ϕ even slightly greater than that for the fast solution will grow toward even larger porosities. Although the maximum ϕ is 1 (lest we have a negative viscosity), solutions with porosities larger than that for the high-porosity/fast solution will undergo a run-away to $\phi = 1$ and hence zero viscosity. Indeed, by inspection of Equation (34), an urealistic solution of ϕ infinitesimally larger than 1 leads to an infinitely large negative growth rate which forces such unrealisic solutions to decay back to $\phi = 1$. In essence, $\phi = 1$ is a stable singularity. In those regions with $\phi = 1$

the strain-rate (which goes as $\tau/(1-\phi)$) will be infinite. However, the size of any zero-viscosity zone is of finite width since it is entirely dependent on the initial porosity field; it will be as large as any region whose initial porosity exceeded that for the high-porosity/fast steady solution and thus grew to $\phi = 1$. Thus although the strain-rate might be heterogeneous, the shear zone does not necessarily self-localize, although the infinite strain-rates require the velocity drop across a zero-viscosity zone to be infinite. Finally, if $\tau > 1/2$, there are no possible steady solutions (see Eqn. 33 and Fig. **1**) and the entire system goes to $\phi = 1$, i.e., the entire layer undergoes a runaway and has an infinite velocity drop across it.

To put some of these dimensionless results in a physical perspective, we can try to redimensionalize the critical stress $\tau = \frac{1}{2}$ (below which there is shear-localization since two strain-rate solutions are permitted). The simple damage theory is idealized but we can relate some of the constants in the scaling equation Equation (31) to physical parameters. First, the partitioning fraction f is likely to be of order 0.1 (Ricard and Bercovici 2002), and λ is likely to be near unity. We can assume a very high lithospheric viscosity of $\mu_0 \approx 10^{25}$ Pa s (Beaumont 1976; Watts et al. 1982), and that background porosity $\Phi_0 \ll 1$. The quantitiy B is more difficult to quantify; it has units that represent the loss of energy density ($\mathrm{J/m^3}$) per second. The energy density is likely given by surface energy on cracks, which in terms of volumetric energy density will be surface energy Γ–typically of order 1-100 $\mathrm{J/m^2}$ for crack surfaces (Jaeger and Cook 1979; Cooper and Kohlstedt 1982; Atkinson 1987; Atkinson and Meredith 1987)– times void or crack curvature c (the inverse of void or crack size which is typically 100-1000 $\mathrm{m^{-1}}$). The loss rate of this energy is unclear but we will assume that is controlled by loss of void-filling material, namely water, through Darcy-type flow; in this case the flux rate (Darcy velocity) of fluid is of the order $V = k_\phi \rho_w g/\mu_w$, where k_ϕ is permeability (of order 10^{-14} $\mathrm{m^2}$ for porous rocks), ρ_w is water density (1000 $\mathrm{kg/m^3}$), g is gravity, and μ_w is water viscosity (10^{-3} Pa s). The time-scale for energy loss will be typically L/V where L is the length-scale of the shear-zone (1-10 km), and thus B will scale as $\Gamma c V/L$. Given these values, the critical dimensional stress σ from Equation (31) is of the order several 100 to 1000 MPa, which is indeed typical of or larger than tectonic stresses. Thus we can speculate that tectonic stresses are sufficient to induce localization with this damage mechanism.

Grainsize feedback

Grainsize reduction is an important cause for shear localization. The association of shear localization and grainsize reduction is evident in mylonite shear zones (White et al. 1980; Jin et al. 1998). However, the link between grainsize reduction and shear localization is not clearly understood. The way in which grainsize is controlled during deformation is more complicated than other variables such as temperature. In fact, some recent analyses underscored the difficulties in explaining shear localization through grainsize reduction (Bresser et al. 2001; Montési and Zuber 2002), suggesting a need for more complete analysis of this problem. This section reviews some key concepts in grainsize sensitivity of deformation with the emphasis on the processes of dynamic recrystallization.

Grainsize controls the rheology through two contrasting ways. Under low temperature conditions where dislocation recovery and diffusion do not occur, grainboundaries act as a barrier for dislocation motion and the presence of many grainboundaries causes hardening (the Hall-Petch effect; see Cottrell 1953). In contrast, when diffusion and resultant dislo-

cation recovery become effective (at high temperature T, i.e., exceeding roughly 50% of the melting temperature), then a smaller grainsize leads to weakening because deformation by diffusive mass transport occurs more efficiently for smaller grain sizes. Under most tectonic conditions except the shallow lithosphere, diffusive mass transfer is likely to be important, and we consider the effects of diffusion creep here. For simplicity, we assume (as in the previous sections) that viscosity depends only on grainsize a and strain-rate, i.e.,

$$\mu = \mu(a, \dot{\varepsilon}) = \mu_r \left(\frac{a}{a_0}\right)^m \left(\frac{\dot{\varepsilon}}{\dot{\varepsilon}_0}\right)^{\frac{1-n}{n}} \tag{35}$$

where $m = 2 - 3$ and $n = 1$ for diffusion creep, and $m \approx 0$ and $n = 3 - 5$ for dislocation creep; a_0 is a reference grainsize and $\dot{\varepsilon}_0$ is the reference strain-rate, both of which are defined below. The rheological law Equation (35) prescribes dependence of viscosity on grainsize and strain-rate, although strictly speaking these effects do not occur simultaneously since grainsize dependence occurs in diffusion creep, and strain-rate dependence occurs in dislocation creep. Moreover, one of the dominant processes leading to grainsize reduction, namely dynamic recrystallization, occurs only in the dislocation-creep regime, and thus the feedback between grainsize reduction (while in the dislocation-creep regime) and grainsize-weakening (while in the diffusion-creep regime) only occurs if the material essentially experiences both creep regimes. This would seem to constrain the feedback mechanism to only be effective near the transition between creep regimes. However, the actual rheology of the material is complicated because it is essentially composed of two phases, i.e., coarse-grained strong matrix (which deforms by dislocation creep) and fine-grained weak regions (deforming by diffusion creep). The flow law parameters such as n and m in such a two-phase material are not well known but are likely to be between those for dislocation and diffusion creep. Therefore when deformation reduces the grainsize, there is a feedback mechanism that could causes self-weakening and shear localization.

There are several processes by which grainsize evolves. The first is dynamic recrystallization wherein gradients in dislocation density drive formation of new grainboundaries and/or mobilization of existing boundaries leading to the modification of grainsize. Evidence of dynamic recrystallization is ubiquitous in naturally deformed rocks (Urai et al. 1986). The second process involves chemical reactions, including phase transformations (Furusho and Kanagawa 1999; Karato et al. 2001; Rubie 1983, 1984; Stünitz and Tullis 2001). In both cases, the kinetics of nucleation and growth controls the grainsize during deformation or chemical reactions, whereas after the completion of these processes, grain growth, through the reduction of grain-boundary surface energy, plays an important role when the grainsize is small enough. Whether grainsize modification causes shear localization depends on the competition between the weakening effect due to grainsize reduction and the hardening effect due to graingrowth, the details of which are specific to the particular processes involved. Here we consider the effects of grainsize evolution during dynamic recrystallization. In this case, and in the context of our simple-shear flow model, grainsize evolution may be described by

$$\frac{\partial a}{\partial t} = -\frac{\dot{\varepsilon}}{\varepsilon_r}(a - a_0) + \frac{K}{p a^{p-1}} \tag{36}$$

(Karato 1996; Kameyama et al. 1997) where the first term represents the effect of dynamic recrystallization on grainsize and the second term the effect of graingrowth; $\varepsilon_r \approx 1$ is

the strain needed to complete dynamic recrystallization (Karato et al. 1980); K is a rate constant for graingrowth; $p = 2 - 3$ such that grain growth is fastest for smaller grains when grain-boundary surface energy is large and diminishes as grains increase in size; and a_0 is the equilibrium value of a if there were no grain-growth and is in effect the grainsize at which dynamic recrystallization is completed. This grainsize a_0 may be determined by the nucleation-growth and impingement of growing subgrains on one another (Derby and Ashby 1987), or by subgrain rotation and dislodgement under deformation (Shimizu 1998). The implicit assumptions behind Equation (36) are, first, that grainsize reduction and graingrowth occurs simultaneously, and, second, that the time scale to obtain a short-term equilibrium grainsize a_0 is significantly smaller than the time scale for graingrowth (therefore a_0 is assumed to be a constant).

As in previous sections, we nondimensionalize Equation (36) by defining $a = a_0\alpha$, $t = \frac{pa_0^p}{K}t'$, and $\dot{\varepsilon} = \frac{K\varepsilon_r}{pa_0^p}\dot{\varepsilon}'$ and thus obtain (dropping the primes for simplicity)

$$\frac{\partial\alpha}{\partial t} = -\dot{\varepsilon}(\alpha - 1) + \alpha^{1-p} \tag{37}$$

Similarly, the constitutive law $\sigma = 2\mu\dot{\varepsilon}$ becomes, using Equation (35),

$$\tau = \alpha^m \dot{\varepsilon}^{1/n} \tag{38}$$

where

$$\tau = \frac{\sigma p a_0^p}{2\mu_r \varepsilon_r K} \tag{39}$$

In steady state, Equation (37) leads to

$$\dot{\varepsilon} = \frac{\alpha^{1-p}}{\alpha - 1} \tag{40}$$

in which case we can re-write Equation (38) as

$$\tau = \left(\frac{\alpha^{nm+1-p}}{\alpha - 1}\right)^{1/n} \tag{41}$$

We can therefore display an effective constitutive law, as we did previously, by writing τ as a function of $\dot{\varepsilon}$ parametrically through α, as shown in Figure **1**. There is no steadystate for $\alpha < 1$ where grainsize increases both by dynamic recrystallization and by graingrowth (assuming that both the imposed τ and the resulting $\dot{\varepsilon}$ are > 0). We will thus consider only the case $\alpha > 1$, that is when an initially large grainsize is reduced by deformation.

For sufficiently large m (i.e., sufficient grainsize dependence), the effective constitutive law is similar to that for the thermal-feedback case in which there is a region at low strain-rates whereby stress decreases with strain-rate (the "slip" regions), and a region at higher-strain rates whereby stress increases gradually. The stress-loss region is, as discussed before, an apparent feature of shear-localizing mechanisms. In contrast to the other feedback mechanisms, however, there is no finite region at low-strain-rates where stress increases sharply with strain-rate. Instead the peak strength occurs at zero strain-rate, which is similar to true stick-slip behavior whereby the "stick" response involves no motion until

a peak or yield stress is achieved, after which there is progressive loss of strength (i.e., failure ensues).

The stick-slip region only exists when there is a minimum stress in the effective constitutive curve (see Fig. **1**) which means that somewere on the curve

$$\frac{d\tau}{d\dot{\varepsilon}} = \frac{d\alpha}{d\dot{\varepsilon}}\frac{d\tau}{d\alpha} = \frac{1}{n}\left(\frac{\alpha^{nm+1-p}}{\alpha-1}\right)^{\frac{1-n}{n}} \alpha^{nm}\frac{1-(nm-p)(\alpha-1)}{1+p(\alpha-1)} = 0 \tag{42}$$

For $m = 0$ (i.e., no grainsize dependence) there can be no stress minimum and the constitutive curve has the appearance of a simple power-law relationship. For $m > 0$, the minimum occurs at $\alpha = 1 + \frac{1}{nm-p}$. Since we require $\alpha > 1$ then $nm > p$; therefore if, for example, $n = 3$ and $p = 3$ then even linear grainsize dependence $m = 1$ is not sufficient to give a stick-slip effect and the constitutive curve again looks like the case for $m = 0$ (see Fig. **1**). For parameter combinations in which $nm > p$, stick-slip behavior can occur.

One should note, however, that in cases where stick-slip behavior occurs the stress spuriously goes to infinity as strain-rate goes to zero (see Fig. **1**). This is an artifact of the model in that as grainsize α goes to infinity (associated with $\dot{\varepsilon} \to 0$; see Eqn. 40) the grain-size dependence of stress is assumed to persist (leading to $\tau \to \infty$; see Eqn. 41) even though it should not (i.e., dislocation creep must dominate). Althought beyond the scope of this paper, a correction to this artifact, such as a grainsize-dependence index m that is itself grainsize-dependent (i.e., vanishes at some finite grainsize), would likely mitigate this effect and result in proper stick-slip curves similar to those shown for the other mechanisms of Figure **1**.

The solutions for α in the steady-state system are the roots of Equation (41), which are shown in Figure **2**. There are two solutions if the imposed stress is greater than the minimum stress

$$\tau > \tau_{min} = \left(\frac{(nm-p+1)^{nm-p+1}}{(nm-p)^{nm-p}}\right)^{1/n} \tag{43}$$

The minimum stress τ_{min} is only guaranteed to exist for $nm > p$. For reasonable values of n, m and p, this minimum stress is $2 < \tau_{min} < 3$ which corresponds to 2-300 MPa for $\mu_r = 10^{18}$ Pa s and $\dot{\varepsilon}_0 = 10^{-10} - 10^{-12}$ s^{-1}. One of the solutions is very near $\alpha = 1$ (the equilibrium grainsize without graingrowth) and the other at large grainsize (Fig. **2**). As stress increases and one moves further away from the minimum stress τ_{min}, the small grainsize solution decreases whereas the latter increases. For stresses less than τ_{min} , there are no steady-state solutions.

The existence of at least two steady solutions, which leads to two possible strain-rates as shown in Figure **1**, is a minimum requirement for localization to occur in this, as well as other previously discussed decay-loss systems. Without two possible solutions, then only one strain-rate exists and then the entire shear-layer has uniform shear. If two strain-rates are possible, then the layer can have low-strain-rate regions surrounding high-strain-rate regions which would represent the zones of shear-localization.

However, an important difference between the grainsize feedback mechanism and the other two we have discussed (thermal and damage) is that the shear-localization regime exists for stresses greater than a minimum stress, i.e., it is a high-stress phenomenon; the

other two mechanisms occur for stresses less than a maximum, i.e., they are low-stress phenomena.

The stability of these steady solutions is determined by combining Equation (37) and Equation (38) to obtain

$$\frac{\partial \alpha}{\partial t} = \tau^n \frac{1-\alpha}{\alpha^{nm}} + \alpha^{1-p} \tag{44}$$

whose phase-plot (i.e., $d\alpha/dt$ versus α) is displayed in Figure **3** for various values of stress τ. For a stress higher than the τ_{min} (such that two steady solutions are realized), the steady solution for the small grainsize is stable (the slope of the phase-plot curve is negative at the steady solution, i.e., where it crosses the line $d\alpha/dt = 0$) whereas the solution for large grainsize is unstable. For an unstable grainsize, shear localization occurs through bifurcation: grains larger than the unstable equilibrium size grow to make materials stronger (i.e., yield smaller strain-rate) and grains smaller than that size make materials softer hence yield higher strain-rates. For stresses smaller than τ_{min} there are no steady solutions and the grainsize everywhere grows indefinitely; in this case, stresses are too small to provide significant dynamic recrystallization and thus grain growth dominates. Therefore a necessary condition for shear localization, in this grainsize model, is given by Equation (43). However, certain values of n, m and p (in particular that $nm > p$) are also necessary to guarantee the existence of a minimum stress.

The degree to which shear localization develops depends not only on the stress but also on the viscosity contrast between the two regions which depends, in turn, on the magnitude of stress as well as temperature. The degree of localization will be higher for higher stresses and lower temperatures because of the smaller grainsize at higher stress, and because of the smaller activation energy for diffusion creep than that for dislocation creep in many minerals (Jin et al. 1998).

Note that if the presence of short-term equilibrium is ignored (i.e., $a_0 = 0$), then Equations (37) and (38) are reduced to

$$\frac{\partial \alpha}{\partial t} = -\dot{\varepsilon}\alpha + \alpha^{1-p} \tag{45}$$

and

$$\tau = \alpha^{\frac{nm+1-p}{n}} \tag{46}$$

respectively. Equation (46) has only one solution and hence no bifurcation and resultant shear localization will occur. We conclude therefore that the presence of a short-term, quasi-equilibrium state is crucial for the development of instability and localization associated with grainsize evolution due to dynamic recrystallization. Under these conditions, a single stress can allow two different grainsizes and thus heterogeneous strain-rate leading to localization; in essence, the material is composed of two "phases", one with a small grainsize (a weak phase) and the other with large grainsize (a strong phase), and therefore the presence of twophases is essential for the shear localization. This conclusion is consistent with the field and laboratory observations where the transient stage of dynamic recrystallization is characterized by a bimodal distribution of grainsize (Jin et al. 1998; Lee et al. 2002).

Various simplifying assumptions have been made that need to be discussed here. First, we assumed the presence of two time scales to control the grainsize. They correspond to two physical processes; one is the smallscale balance between growing grainboundaries and impingement (Derby and Ashby 1987) or local balance caused by subgrainrotation (Shimizu 1998), and another is the largerscale balance in regions of complete recrystallization. When the stress is low and diffusion creep dominates in these regions, then grain-growth driven by grain-boundary surface energy will occur, which would be balanced with grainsize reduction by dynamic recrystallization. The latter, longer-scale balance model, is similar to that by Bresser et al. (1998), but is different from their model. The De Bresser model assumes that the strain-rates due to diffusion creep and dislocation creep balance. There is no reason for the strain-rates of these processes to balance because they are independent processes (Frost and Ashby 1982; Poirier 1985), although grain-growth and grainsize reduction may balance under some limited conditions. Second, we assumed that grainsize reduction (by dynamic recrystallization) and graingrowth occur simultaneously. Strictly speaking, this is not correct because, for a given grainboundary, either dislocation density contrast or grainboundary curvature imbalance contributes to grainboundary migration. However, Equation (36) captures some physics to the extent that smaller grains tend to grow by grainboundary energy driven migration and larger grains tend to reduce their size through grainboundary migration driven by dislocation density heterogeneity. Third, the rheology of a material during the transient stage of dynamic recrystallization is likely to be sensitive to the geometry of a weaker (finegrained) material. When the weaker material assumes a connected network, then a significant reduction in strength occurs, which is likely to lead to unstable localized deformation (Handy 1994). This is analogous to the brittle fracture where the formation of interconnected cracks through crack-crack interaction is the key to the instability (e.g., Paterson 1978). Such an aspect is not included in the present analysis, but is starting to be approached by various damage theories, which is discussed below. Further refinement of the model is needed to treat these details to better understand the role of dynamic recrystallization in shear localization.

The degree of localization by this mechanism may be limited and dependent on the temperature. For example, for olivine-rich regions, when the initial grainsize is approximately 3 mm and a stress pulse of approximately 100 MPa is applied at temperatures around 1100 K, then the viscosity contrast between the coarse and finegrained portions (at the same stress) is $10^2 - 10^3$ but virtually no weakening would occur at $T > 1500$ K. Therefore shear localization due to this mechanism can occur only in the relatively shallow portions of the lithosphere. However, even at relatively low temperatures, extreme localization would be difficult with this mechanism alone. A combination of grainsize reduction with other mechanisms may be needed for extreme localization. Jin et al. (1998) reported evidence that localization caused by grainsize reduction led to shear melting that resulted in extreme localization (faulting).

The analyses by Braun et al. (1999) and Frederiksen and Braun (2001) also include the effects of transient behavior associated with grainsize reduction. In particular, the treatment by Frederiksen and Braun (2001) is equivalent to a two-phase behavior but the microscopic basis for the two-phase behavior was not examined in their paper.

Finally, other processes such as phase transformations (or chemical reactions) also lead to grainsize reduction and resultant rheological weakening and shear localization (Furusho and Kanagawa 1999; Stünitz and Tullis 2001) (see also Green and Marone, this volume).

The key concept in such a case is the degree of grainsize reduction associated with a phase transformation or chemical reaction and the enhancement of transformation by deformation or vice versa. Although, a quantitative model has been developed for the grainsize reduction due to a phase transformation (Riedel and Karato 1997), the understanding of deformation-transformation (or deformation-chemical reaction) interaction remains qualitative (Green and Burnley 1989; Kirby 1987).

Thermal and simple-damage feedbacks with diffusive-loss healing

Here we consider the nature of shear-localization when the loss mechanism is diffusive, i.e., dependent on gradients of gradients (or "curvature") in the state variable Θ. This loss mechanism is only relevant for the thermal feedback mechanism and perhaps the damage mechanism if the void-filling fluid undergoes chemical diffusion or hydrological conduction (i.e., spreads out to mitigate fluid pressure gradients). The mechanism is not relevant for the grainsize feedback mechanism. In this case, the governing evolution equations for temperature and porosity are similar enough that we can write them with one equation:

$$\rho c \frac{\partial \Theta}{\partial t} = k \frac{\partial^2 \Theta}{\partial y^2} + 2 f \mu(\Theta, \dot{\varepsilon}) \dot{\varepsilon}^2 \tag{47}$$

where Θ is either temperature or porosity, k is a conductivity (thermal, chemical or hydrological), and $f = 1$ for the thermal mechanism, or $0 < f < 1$ for the damage mechanism.

We can solve for the steady-state structure of Θ (in the 0-D examples, this structure was determined by the initial conditions) and thus the velocity field $u(y)$ as well. As with the previous examples using our simple-shear-layer thought-experiment, while shear stress is a constant σ across the layer, Θ is not necessarily so, and thus strain-rate is possibly variable. In terms of the shear-rate $\partial u/\partial y$, the constitutive law leads to

$$\frac{\partial u}{\partial y} = \frac{\sigma}{\mu(\Theta, \partial u/\partial y)} \tag{48}$$

We consider only the steady limit of Equation (47) which is

$$0 = k \frac{\partial^2 \Theta}{\partial y^2} + \tfrac{1}{2} f \mu(\Theta, \partial u/\partial y) \left(\frac{\partial u}{\partial y} \right)^2 \tag{49}$$

In addition to assuming that the channel's top and bottom boundaries (at $y = \pm L$) have equal and opposite motion, we also prescribe them to be held at a constant temperature or porosity Θ_0. Given the symmetry of the problem we assume that at $y = 0$ the velocity u is zero, and Θ is at its maximum (i.e., $\partial\Theta/\partial y = 0$ at $y = 0$). Given these boundary conditions, we can solve Equation (48) and Equation (49) to infer the structure of shear localization across the channel.

We again consider two different viscosity laws, i.e., Arrhenius for the thermal feedback, and linear for the damage feedback, each of which requires a slightly different scaling analysis, and significantly different analytic solutions.

Thermal feedback. Here we examine our basic feedback mechanism using the thermally activated Arrhenius power-law viscosity. Given the constant stress σ across the layer, the stress-strain-rate relation leads to (using Eqn. 9 and Eqn. 48)

$$\frac{\partial u}{\partial y} = 2 \left(\frac{\sigma}{A} \right)^n e^{-\frac{H}{R\Theta}} \tag{50}$$

and a steady heat equation (again using Eqn. 9 and Eqn. 49)

$$0 = k\frac{\partial^2 \Theta}{\partial y^2} + A\left(\frac{1}{2}\frac{\partial u}{\partial y}\right)^{\frac{n+1}{n}} e^{\frac{H}{nR\Theta}} \tag{51}$$

where we assume that all deformational work goes into viscous heating and thus $f = 1$. Again using the nondimensionalizing scheme described previously, where now the temperature and velocity scales are $\Theta^* = H/R$ and $U^* = 2L\left(\frac{kH}{2L^2RA}\right)^{\frac{n}{n+1}}$, Equation (50) and Equation (51) become

$$\frac{\partial u}{\partial y} = \tau^n e^{-\frac{1}{\theta_0+\theta}} \tag{52}$$

$$0 = \frac{\partial^2 \theta}{\partial y^2} + \tfrac{1}{2}\tau^{n+1} e^{-\frac{1}{\theta_0+\theta}} \tag{53}$$

where now

$$\tau = \sigma\left(\frac{2L^2R}{A^n kH}\right)^{\frac{1}{n+1}} \tag{54}$$

and $\theta_0 = R\Theta_0/H$ is the dimensionless boundary temperature. Again, τ is the dimensionless stress, and as with the 0-D decay-loss cases, both n and θ_0 appear in the dimensionless equations. (Although θ_0 could be absorbed into the differential equation readily by defining a variable $\vartheta = \theta_0 + \theta$, it would simply reappear in the boundary conditions.)

Multiplying both sides of Equation (53) by $2\partial\theta/\partial y$ and integrating we arrive at

$$\frac{\partial \theta}{\partial y} = \pm\tau^{\frac{n+1}{2}}\sqrt{\gamma^2 - F(\theta_0+\theta)} \tag{55}$$

where

$$F(\psi) = \int e^{-1/\psi} d\psi = \psi e^{-1/\psi} - \mathrm{Ei}(1, 1/\psi) \tag{56}$$

in which ψ is a dummy variable and

$$\mathrm{Ei}(m, x) = \int_1^\infty t^{-m} e^{-xt} dt \tag{57}$$

is the error integral. We can find solutions to (55) that are parametric in the peak "temperature" θ_{max} which occurs at $y = 0$. First, since $\partial\theta/\partial y = 0$ at $y = 0$ (where $\theta = \theta_{max}$) then we obtain a relation for the integration constant γ:

$$\gamma^2 = F(\theta_0 + \theta_{max}) \tag{58}$$

which can be solved numerically for γ given a θ_0 and θ_{max}. Next, Equation (55) can be integrated from $y = -1$ to an arbitrary $y \le 0$, and/or from $y = 1$ to any $y \ge 0$ to obtain

$$\int_0^\theta \frac{d\theta'}{\sqrt{\gamma^2 - F(\theta_0+\theta')}} = \tau^{\frac{n+1}{2}} \left\{ \begin{array}{ll} 1+y, & \text{for } y \le 0 \\ 1-y, & \text{for } y \ge 0 \end{array} \right\} = \tau^{\frac{n+1}{2}}(1 - |y|) \tag{59}$$

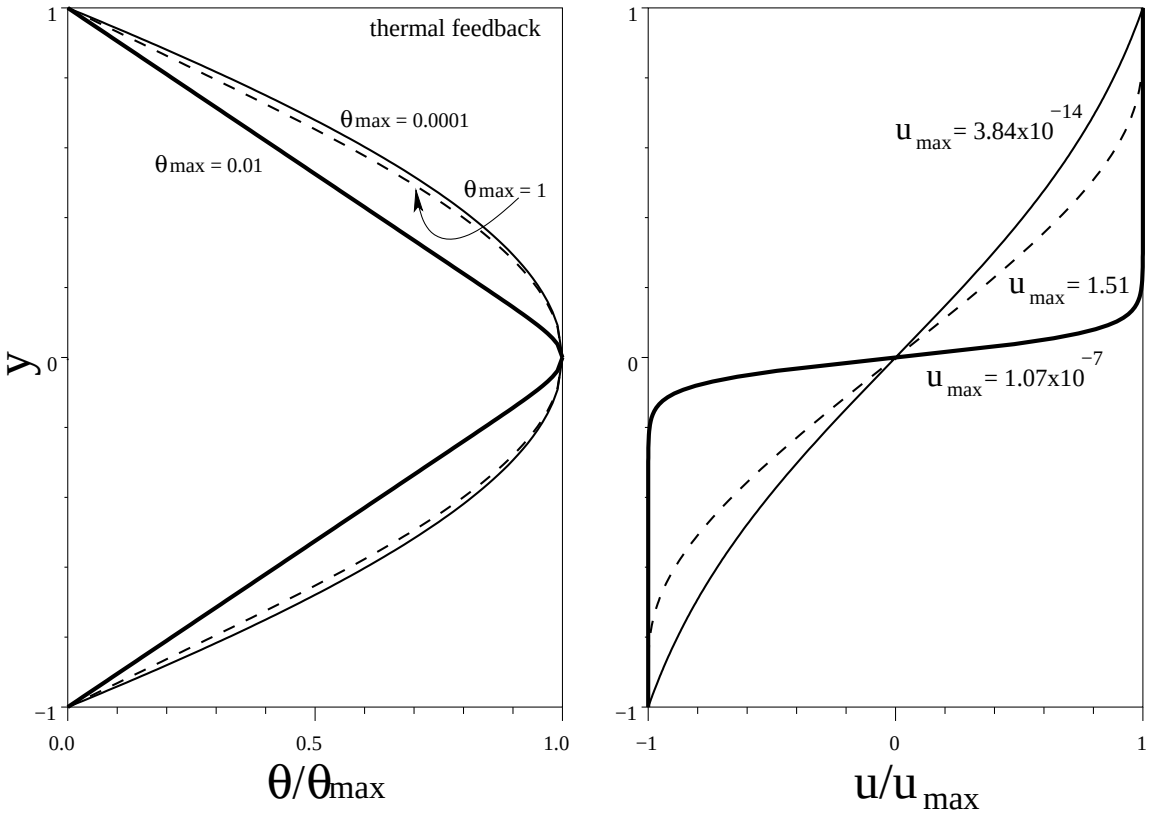

Figure 4: Temperature (θ) and velocity (u) versus distance across the sheared layer y, for the thermal feedback mechanism with diffusive loss and three different maximum temperature anomalies θ_{max} (indicated) and a boundary temperature $\theta_0 = 0.01$. Only intermediate temperatures ($\theta_{max} \approx \theta_0$, the thick solid curve in each frame) generate localization while cold ($\theta_{max} \ll \theta_0$, the thin solid curves) and hot ($\theta_{max} \gg \theta_0$, dashed curves) temperatures generate more distributed and nearly constant shear. Curves are normalized by their maxima (values indicated).

where we have used the plus sign in Equation (55) for $y < 0$ and the minus for $y > 0$ because we assume the temperature increases from the boundary at $y = -1$ to its maximum at $y = 0$ and then decreases again toward the boundary at $y = 1$. At $y = 0$ equation Equation (59) yields a relation for τ as a function of θ_{max}:

$$\tau^{\frac{n+1}{2}} = \int_0^{\theta_{max}} \frac{d\theta'}{\sqrt{\gamma^2 - F(\theta_0 + \theta')}} \tag{60}$$

Lastly, Equation (52) can be integrated to obtain

$$\begin{aligned} u &= u_0 + \tau^n \int e^{-\frac{1}{\theta_0+\theta}} dy \\ &= u_0 - \mathrm{sgn}(y)\tau^{\frac{n-1}{2}} \int \frac{e^{-\frac{1}{\theta_0+\theta}}}{\sqrt{\gamma^2 - F(\theta_0+\theta)}} d\theta \\ &= \mathrm{sgn}(y) 2\tau^{\frac{n-1}{2}} \sqrt{\gamma^2 - F(\theta_0+\theta)} \end{aligned} \tag{61}$$

where we have used the fact that $u = 0$ at $y = 0$ to eliminate u_0.

Both temperature and velocity fields for this case are shown in Figure **4** for various temperature-anomaly maxima θ_{max}. Localization only occurs for relatively cold boundaries

(in the cases shown, $\theta_0 = 0.01$); with much hotter boundaries, there is never any significant localization since the entire viscosity field is near the minimum value given by the limit $\Theta \to \infty$ and so thermal perturbations have little effect.

Even with cold boundaries, localization only occurs for a finite range of peak "temperature" θ_{max}. If θ_{max} is too small (in particular $\ll \theta_0$) then the temperature is nearly constant across the layer and thus the viscosity field is approximately uniform and very large; this then leads to effectively Newtonian, constant-viscosity behavior with uniform shear. If θ_{max} is too large (i.e., $\gg \theta_0$) then most of the viscosity field (instead of just a narrow portion) approaches the low-viscosity limit at $\Theta \to \infty$ and thus viscosity and shear are mostly uniform. For $\theta_{max} \sim \theta_0$, the thermal anomalies are neither insignificant nor so large as to dominate the entire viscosity field, and thus one can obtain significant viscosity variations and shear localization across the layer. This result somewhat corresponds to the curve shown in Figure **1** wherein the "stick-slip" behavior for the Arrhenius mechanism occurs only over a finite parameter range (in those cases, over a finite range of strain-rates) outside of which behavior is mostly like that of simple viscous fluids.

Simple-damage feedback. For the simplified damage feedback we again use the simplified linearly temperature-dependent viscosity law $\mu = \mu_r(1 - \lambda\Theta)$, use $f < 1$ and rewrite our dependent and independent variables in terms of natural scales, i.e., $y = Ly'$, $\Theta = \Theta_0 + \Theta^*\theta$, and $u = U^*u'$ where y', θ and u' are dimensionless quantities, and Θ^* and U^* are unknown scales. In this regard, Equation (48) and Equation (49) become

$$\frac{\partial u'}{\partial y} = \left[\frac{\sigma L}{\mu_r(1-\lambda\Theta_0)U^*}\right]\left(1 - \frac{\lambda\Theta^*}{1-\lambda\Theta_0}\theta\right)^{-1} \tag{62}$$

$$0 = \frac{\partial^2\theta}{\partial y^2} + \tfrac{1}{2}\left[\frac{\mu_r(1-\lambda\Theta_0)(U^*)^2}{k\Theta^*}\right]\left(1 - \frac{\lambda\Theta^*}{1-\lambda\Theta_0}\theta\right)^{-1}\left(\frac{\partial u'}{\partial y}\right)^2 \tag{63}$$

Choosing $\Theta^* = (1-\lambda\Theta_0)/\lambda$, $U^* = \sqrt{\frac{k}{\mu_r\lambda}}$, then Equation (62) and Equation (63) become (after dropping the primes)

$$\frac{\partial u}{\partial y} = \frac{\tau}{1-\theta} \tag{64}$$

$$0 = \frac{\partial^2\theta}{\partial y^2} + \frac{\tau^2}{2}\frac{1}{1-\theta} \tag{65}$$

where we have used Equation (64) to eliminate $\partial u/\partial y$ from Equation (65), and

$$\tau = \sigma\sqrt{\frac{\lambda L^2}{\mu_r(1-\lambda\Theta_0)^2 k}} \tag{66}$$

is our only free parameter and, again, represents a dimensionless imposed stress. To solve Equation (65) we multiply both sides by $2\partial\theta/\partial y$ to arrive at

$$0 = \frac{\partial}{\partial y}\left(\frac{\partial\theta}{\partial y}\right)^2 = \tau^2\frac{\partial}{\partial y}\ln(1-\theta) \tag{67}$$

which leads to

$$\int \frac{d\theta}{\sqrt{\gamma^2 + \ln(1-\theta)}} = \pm\tau(y - y_0) \tag{68}$$

where γ^2 and y_0 are integration constants; moreover, the plus sign on the right side corresponds to $y < 0$, and the minus sign to $y > 0$ since we expect θ to increase from 0 at $y = -1$ to a maximum at $y = 0$ and and then decrease to 0 again at $y = 1$. The above integral can be solved by making the substitution $\psi = \sqrt{\gamma^2 + \ln(1-\theta)}$ which eventually leads to the the implicit solution (i.e., y as a function of θ)

$$e^{-\gamma^2}\mathrm{erfi}(\sqrt{\gamma^2 + \ln(1-\theta)}) = \pm\frac{\tau}{\sqrt{\pi}}(y_0 - y) \tag{69}$$

where erfi is the imaginary error function $\mathrm{erfi}(x) = -i\mathrm{erf}(ix)$ (and by definition $\mathrm{erf}(x) = \frac{2}{\sqrt{\pi}}\int_{-\infty}^{x} e^{-x'^2}dx'$). At $y = -1$ the above equation yields $e^{-\gamma^2}\mathrm{erfi}(\gamma) = \frac{\tau}{\sqrt{\pi}}(y_0 + 1)$ and at $y = +1$ it becomes $e^{-\gamma^2}\mathrm{erfi}(\gamma) = \frac{\tau}{\sqrt{\pi}}(1 - y_0)$; both relations can only be true if $y_0 = 0$. This leads to a transcendental equation for γ

$$\mathrm{erfi}(\gamma) = \frac{\tau}{\sqrt{\pi}}e^{\gamma^2} \tag{70}$$

which generally has two roots, but only for a finite range of τ; there is no solution for γ for $\tau > \tau_c$ where at τ_c the curves (i.e., functions of γ) on each side of Equation (70) just separate, i.e., intersect at one tangent point; this leads to $\mathrm{erfi}(1/\tau_c) = \frac{\tau_c}{\sqrt{\pi}}e^{1/\tau_c^2}$, the solution for which is $\tau_c \approx 1.082$. Again, as shown in the earlier section on damage with decay-loss, this critical stress when redimensionalized will be of the order of 1kbar.

To obtain the velocity field we integrate Equation (64) to obtain

$$u = \tau e^{\gamma^2}\int exp(-[\mathrm{erfi}^{-1}(e^{\gamma^2}\tau y/\sqrt{\pi})]^2)dy = 2\mathrm{erfi}^{-1}(e^{\gamma^2}\tau y/\sqrt{\pi}) \tag{71}$$

where erfi^{-1} is the inverse of the imaginary error function and we have used the condition that $u = 0$ at $y = 0$ to eliminate the integration constant. Evaluating Equation (71) at $y = \pm 1$, and using Equation (70), we find that the velocity at the boundaries is $\pm 2\gamma$; therefore γ represents the boundary or maximum velocity (within a factor or 2). By inspection of the argument to the erfi^{-1} function in Equation (71), it is clear that the width of the shear localization zone is

$$\delta_{sl} = \frac{\sqrt{\pi}}{\tau}e^{-\gamma^2} = \frac{1}{\mathrm{erfi}\gamma} \tag{72}$$

which is an extremely rapidly decreasing function of γ; thus for large γ, δ_{sl} will be extremely small.

That there are two possible values of γ for each $\tau < \tau_c$ means there are two possible porosity and velocity fields, θ and u, for each imposed stress τ. These two solutions have small and large γ which correspond to the low-porosity/slow case (where the viscosity is large but strain-rate low) and a high-porosity/fast case (low viscosity but high strain-rate). That there are no steady-state solutions for $\tau > \tau_c$ is also evident in Figure **1** by the fact that effective constitutive law does not exist for stresses above the stress maximum.

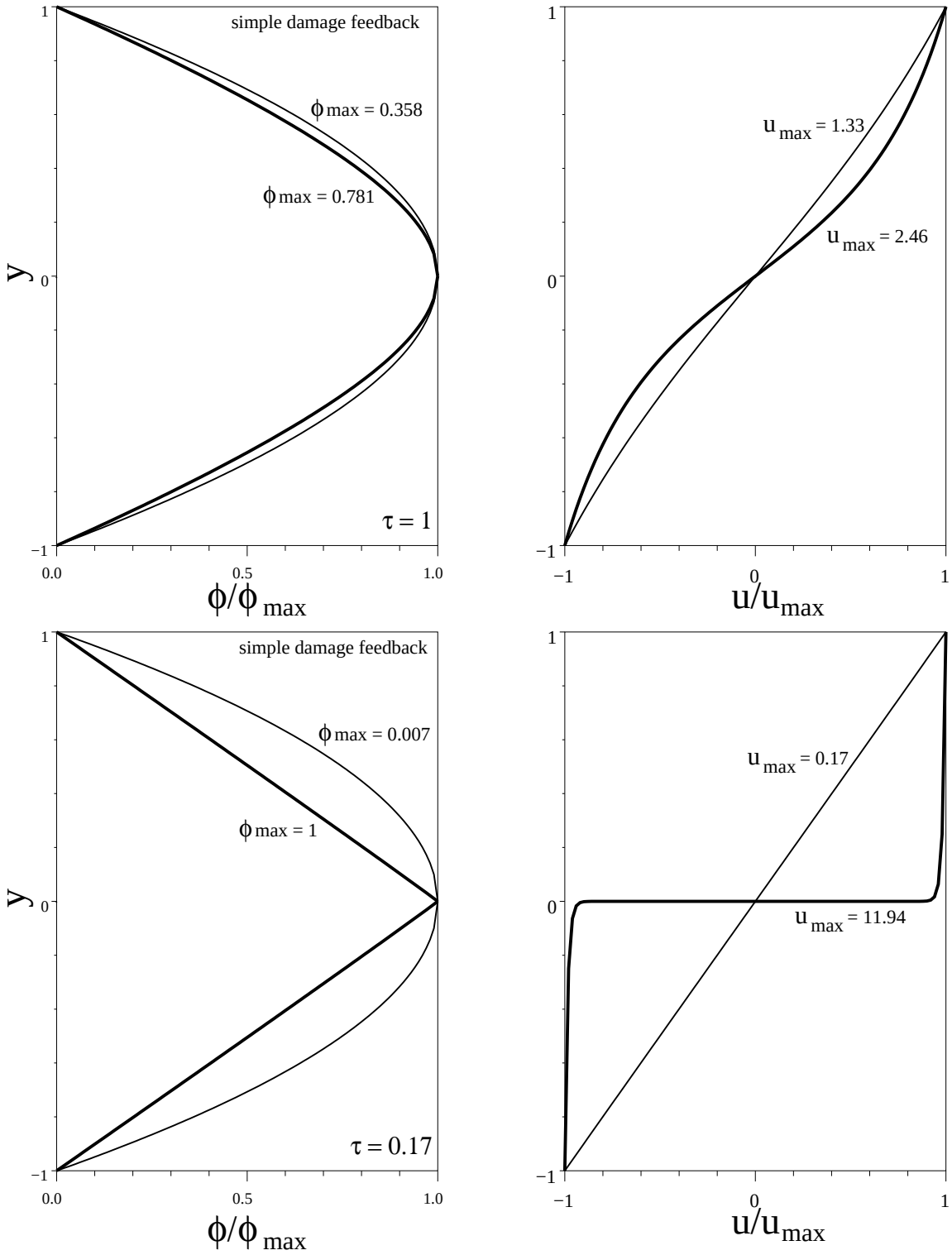

Figure 5: Void fraction or porosity (ϕ) and velocity (u) fields for the simple damage feedback mechanism with diffusive loss and for two different stresses τ (values indicated). Each stress is associated with two possible solutions, the low-porosity/slow case (thin solid line) and the high-porosity/fast (thick solidline) one. Curves are normalized by their maxima (values indicated). See text for discussion.

Figure **5** shows sample solutions for θ and u for various τ; At $\tau \approx \tau_c$ the low-porosity (slow) and high-porosity (fast) solutions coincide and involve relatively weak shear localization. As $\tau \to 0$, the slow solutions approach the constant-viscosity situation in which there is no shear-localization (γ is small and thus δ_{sl} is large), and the fast solutions involve increasingly larger boundary velocities and shear-localization at the midplane $y = 0$ that approaches a nearly fault-like quality (γ is large and thus δ_{sl} is extremely small). It is important to note again that in this case shear localization is associated with decreasing – not increasing – stress τ; i.e., the occurence of shear-localization is associated with a loss of strength whereby the layer is so weakened that even a very high strain-rate involves a small stress.

OTHER CONSIDERATIONS

Two-dimensional examples

Some of the feedback mechanisms discussed herein have been examined in various ways by many authors with regard to lithosphere and mantle dynamics and general rock mechanics (Schubert and Turcotte 1972; Schubert and Yuen 1978; Yuen and Schubert 1977, 1979; Fleitout and Froidevaux 1980; Poirier 1980; Balachandar et al. 1995; Bercovici 1996, 1998) and incorporated in various ways into mantle-convection calculations (Tackley 2000c,d,a; Auth et al. 2002). These applications have been discussed in other reviews in some detail (Bercovici et al. 2000; Tackley 2000b; Bercovici 2003). However, with immediate application to our analysis so far, Bercovici (1998) examined some simple two-dimensional flow calculations using some of the feedback mechanisms discussed above. In those calculations, a thin 2-D horizontal fluid layer (representing the lithosphere) is driven by a source and sink field (representing a mid-ocean ridge and a subduction zone, respectively). The fluid layer experiences the basic feedback mechanisms with either an exponential (e.g., $\mu \sim e^{-\lambda\Theta}$) or a linear viscosity law ($\mu \sim 1 - \lambda\Theta$). The exponential law represents a temperature-dependent viscosity (in fact, it is a semi-linearization of the Arrhenius law, i.e., the argument to the exponential is linearized), while the linear one represents a porosity-dependent law (with a damage feedback in which deformational work generates voids). The goal of the calculation was to see if the various feedback mechanisms could cause the source-sink driven flow to appear plate-like. A perfectly plate like flow would involve localized zones of strike-slip shear, or vertical vorticity, connecting the ends of the sources to the ends of the sinks (Bercovici 1993). In the calculations shown in Figure **6**, the temperature-dependent viscosity law generates very little shear localization and flow that is only weakly plate-like (although, as noted previously, this neglects the likelihood of melting at very high dissipative heating rates), while the linear viscosity law generates a very narrow and intense localization. These more complicated two-dimensional results, therefore, are in keeping with the basic physics discussed with our one-dimensional analysis.

Incorporation of the void-volatile damage theory into two-dimensional convection calculations shows a regime of plate-like behavior involving discrete block-like portions of the cold upper thermal boundary layer and the development of passive spreading centers (Ogawa 2002) and dual low-angle fault-like zones above convergent and divergent zones (Auth et al. 2002). Yet, in fully three-dimensional convection calculations with a visco-plastic lithosphere both the void-volatile effect and stick-slip self-lubrication approach appears to lead to too much damage, causing plate-like regions to go unstable and disintegrate

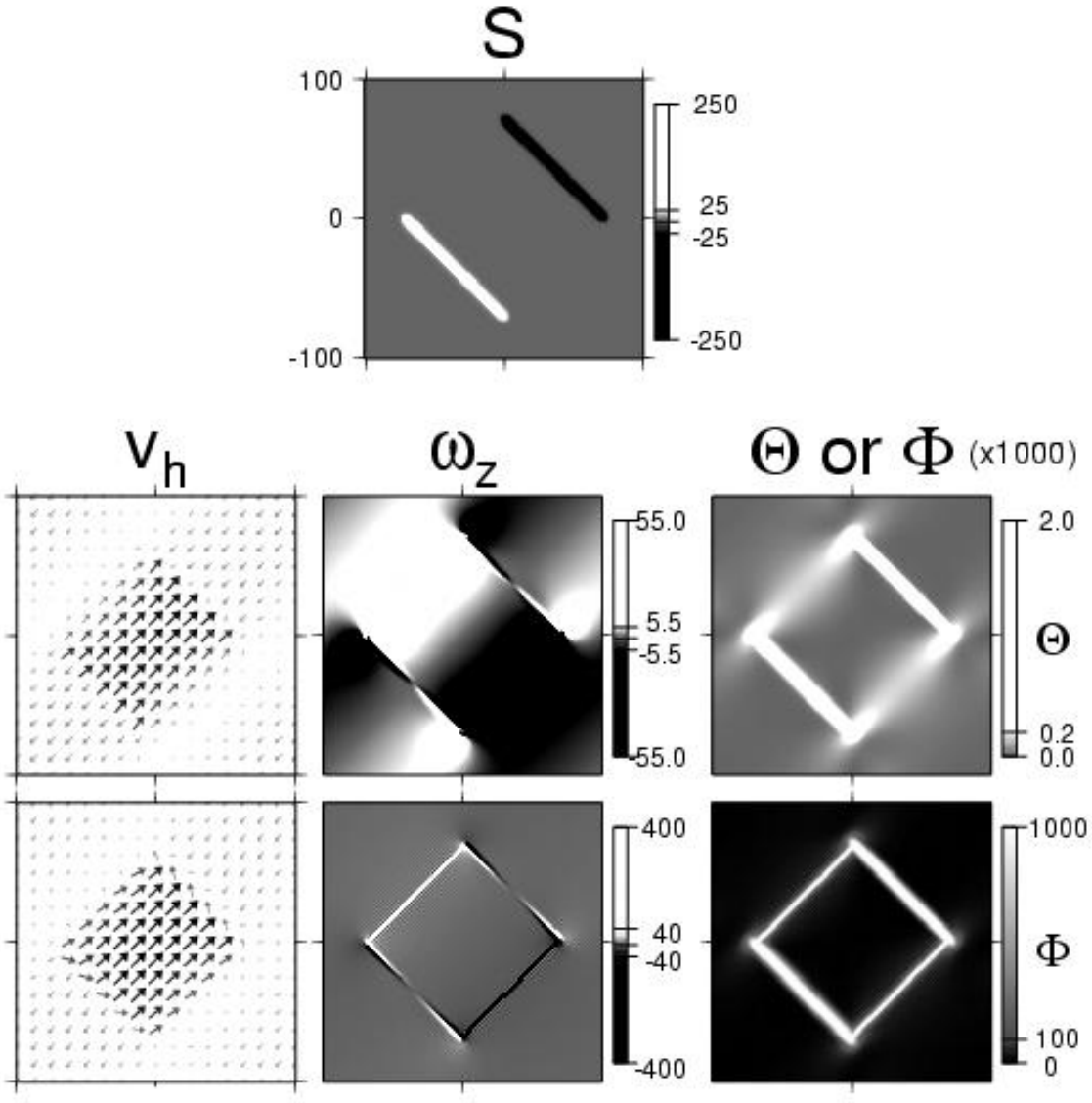

Figure 6: A simple source-sink flow model illustrating two different shear-localization mechanisms, i.e., (1) temperature-dependent viscosity and shear heating, and (2) void-volatile weakening (simple damage). The top frame, labeled S, shows the source-sink field used to drive horizontal flow in a two-dimensional shallow layer; white represents the source and black the sink. The three underlying columns are horizontal velocity v_h (in which gray shading represents velocity magnitude, black being the maximum magnitude); vertical vorticity or rate of strike-slip shear ω_z (white is positive vorticity or left-lateral shear, black is negative vorticity or right-lateral shear), and the scalar field that determines weakening, either temperature Θ or void/volatile volume fraction Φ (white is for large values, and black for small values; the values in the gray scales are multiplied by 1000, as indicated). Without any variable viscosity, the velocity field v_h would look more or less like a dipole field, and there would be no vertical vorticity ω_z. With variable viscosity, the velocity field looks more plate-like and there is signficant vorticity, or toroidal motion, generated. The first row of the 6 lower frames corresponds to the case with temperature-dependent viscosity and shear heating. Softening due to shear heating generates weak zones of strike-slip shear that connect the ends of the source and sink. Although the velocity superficially appears plate-like, in fact significant deformation of the plate-like region is occuring, as depicted in the diffuse zones of vorticity. The temperature field Θ also shows only a weak hot anomaly over the strike-slip zones, and thus a viscosity distribution that is not very plate-like either. With weakening due to creation of voids by damage (bottom row), the velocity field is more plate-like and the vorticity field is similar to what one expects for discontinuous strike-slip faults, i.e., very narrow, intense zones of deformation. The void volume fraction Φ is also very high over the strike slip zones, yielding a contiguous weak boundary surrounding a uniformly strong plate-like area. Modified after Bercovici (1998).

into smaller regions (Tackley 2000d); however, the use of both visco-plasticity and damage schemes is likely redundant since each effect separately represents lithospheric failure mechanisms.

More sophisticated damage theories

The simple void-volatile damage law used by several researchers (Bercovici 1998; Tackley 2000d; Ogawa 2002; Auth et al. 2002) and discussed in this paper, is idealized and is rather unspecific about the intrinsic physics controlling damage and shear localization. In short, while its simplicity is appealing, it is nevertheless ad hoc. A more rigorous damage approach however is difficult to define physically. A signficant body of literature exists on elasto-dynamics damage with applications from metallurgy to earthquakes (Ashby and Sammis 1990; Lemaitre 1992; Lyakhovsky et al. 1997; Krajcinovic 1996, 2000). These models introduce a new thermodynamic field variable (analagous to temperature) called the damage parameter, and given all the new thermodynamic coefficients thus required the models tend toward considerable complexity involving multiple free parameters. Viscous damage theories appropriate to geologic or convective time-scales that are compatible with convection models are rarer. Recently, a first-principles damage approach has been proposed (Bercovici et al. 2001a; Ricard et al. 2001; Bercovici et al. 2001b; Bercovici and Ricard 2003) that combines the essence of fracture mechanics with viscous continuum mechanics. This model is called a "two-phase damage" theory whereby, rather than invoke a new thermodynamic "damage" variable as in the elastodynamics theories, it treats damage through interface and surface thermodynamics. The two-phase damage theory assumes that the existence of a microcrack in a medium entails at least two phases or constituents, i.e., the host phase (the rock) and the void-filling phase (perhaps water). The energy necessary to create the microcrack is–as proposed in Griffiths crack theory (Griffith 1921)–the surface energy on the crack surface, or in the two-phase theory the energy on the interface between phases. Deformational work creates (or is stored as) this interfacial energy by generating more voids, thus inducing weak zones on which deformation concentrates, leading to more damage, void creation, localization and so on.

Preliminary simple calculations show that this mechanism can lead to a spectrum of shear localizing behavior, from more diffuse to very sharp or intense localization (Fig. **7**), in addition to broadly distributed damage when the entire system essentially shatters (Bercovici et al. 2001b; Bercovici and Ricard 2003); the theory has also recently been used to predict shear-enhanced compaction as well as shear-localization (Ricard and Bercovici 2002). However, as simple as the two-phase theory purports to be, it is still rather complicated (as are all two-phase problems) and is thus a work in progress.

SUMMARY AND CONCLUSIONS

That a large amount of deformation on Earth occurs in narrow bands is evidence of the importance of shear-localization in the mantle-lithosphere system. In this review we have discussed some physical and theoretical aspects of various feedback mechanisms that lead to shear-localization. In particular, we examined in some mathematical detail the localization that occurs in a simple shear layer with three different rheological feedback mechanisms. These feedback mechanisms are perhaps the most classical ones considered in lithospheric deformation and include (1) a thermal feedback wherein viscous heating causes softening of the material through a temperature-dependent viscosity; (2) a simple

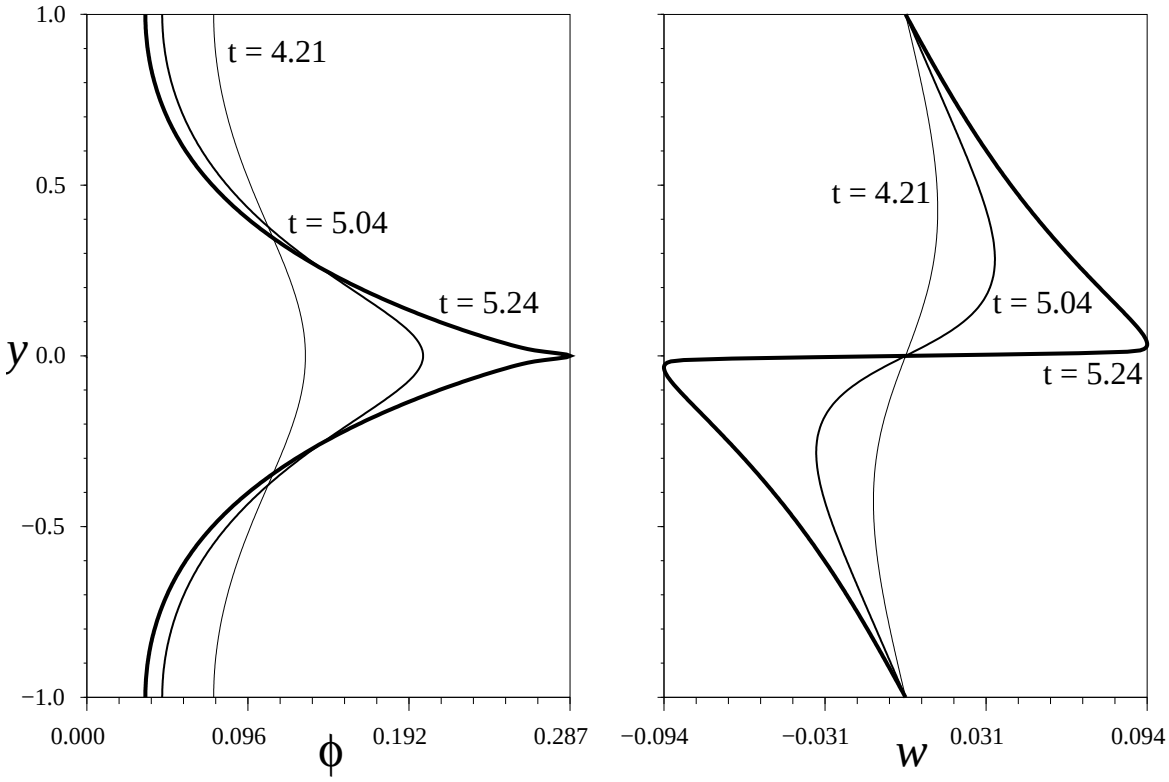

Figure 7: Simple one-dimensional shear-flow calculation demonstrating the two-phase damage theory. Damage occurs as a result of deformational work creating surface energy on void walls (here treated as the interface between two phases, e.g., rock and water); shear localization occurs because the voids cause weak zones on which deformation and further damage concentrates, leading to more voids, etc. The result here is for an infinitely long layer subjected to simple shear by an imposed shear stress (say, by a top boundary at $y = 1$ moving right and the bottom boundary at $y = -1$ moving left). The left panel shows the distribution of void volume density or porosity ϕ across the layer (in the y direction) which indicates the location of the generated weak zone at $y = 0$. The right panel shows the velocity w in the y direction of the matrix (rock) phase; upward motion ($w > 0$) above and downward motion ($w < 0$) below the centerline $y = 0$ indicates the matrix is dilating. The different thickness curves show different times (as indicated) in the calculation. The porosity ϕ evolves to a sharp cusp-like distribution indicating development of a nearly singular (fault-like) weak zone, and the cross-layer velocity w becomes nearly discontinuous at $y = 0$ indicating fault-like dilation. Modified after Bercovici and Ricard (2003).

damage feedback wherein deformational work creates voids that in turn weaken the material; and (3) a grainsize feedback wherein the material grainsize is reduced by dynamic recrystallization (related to propagation of dislocations) which then causes the viscosity to decrease. Each feedback mechanism is associated with a different controlling macroscopic or microscopic variable, which we refer to in general as the state variable; these are, for each feedback, temperature, void fraction (or porosity), and grainsize. We also considered two essential mathematical representations of loss or healing mechanisms, i.e., for each feedback mechanism, cooling, healing of voids, or grain growth and coalescence, respectively. The mathematical representation of loss accounts for either simple decay-type loss (i.e., loss depends only on the local value of the state variable) or diffusive loss (which depends on gradients in the state variable).

In general, the governing equations describe the constitutive relation between stress and strain rate (their ratio in essence being the viscosity), the dependence of viscosity on

state variables (as well as strain-rate, in some cases); the force balance for the material at all points in the shear layer; and the evolution equation for the state variables. These equations in the end provide solutions for how the along-layer velocity (parallel to the boundaries of the shear layer) and the state variables are functions of both time t and the across-layer dimension y; e.g., strong variations in y of velocity and strain-rate as well as strong concentrations of temperature, void-fraction or grainsize, are indications of shear-localization. For our simple shear-layer, stress is constant in y; thus shear-localization, i.e., heterogeneity in strain-rate, only occurs if viscosity is nonuniform in y, which in the end requires nonuniform state variables.

For a decay-type loss mechanism, however, the governing equations make no explicit specifications about change in y; they are zero-dimensional ordinary differential equations with derivatives only in time t. In this case, the spatial structure of shear and the state variables (i.e., y dependence) will be governed by their initial conditions and how their values at each point in the layer evolve independently of any neighboring points (i.e., if there were y derivatives, the evolution of a variable would depend on neighboring values). Localization in this case thus requires the coexistence of at least two independently evolving states: a slow deformation state (involving either cold temperatures, low void-densities or large grainsize and thus high viscosity and low strain rates) and a fast deformation state (low viscosity and high strain rates). A deforming layer that permits both states will, even if the stress across the layer is constant, have hetergenous deformation with the fast deforming zone manifesting itself as the weak shear-localization. If only one deformation state is allowed for a given stress, then deformation is necessarily uniform and there is no localization. Even so, with the decay-type loss mechanism, the width and structure of the localization is not determined by the governing equations but by the initial conditions (which determine which state certain points in the layer evolve toward) and thus these localizations are not truly self-focussing.

In the cases using a decay-type loss, all the different feedback mechanisms generate at least two coexisting states, and thus permit some sort of shear-localization. Since a single stress can be associated with two or more strain-rates, the effective stress–strain-rate constitutive curve is (by definition) non-monotonic; this means that stress does not merely increase with strain-rate as with simple rheological laws but will, over certain regions of strain-rate, actually decrease with increased rate of deformation. The existence of stress-loss regions is associated with stick-slip-type behavior, wherein the "slip" refers to stress loss, and the "stick" to the high stress or resistance region that typically exists at smaller strain-rates.

With the thermal feedback mechanism, three coexisting states are possible if the background temperature (on top of which viscous heating contributes temperature anomalies) is small enough, on the order of (or smaller than) $H/(4R)$ (which corresponds to the condition $\theta_0 < 1/4$) where H is the activation enthalpy and R the gas constant; this is in fact sufficient for any lithospheric temperatures of the order 1000 K. Moreover, the three states only exist if the imposed stress is less than a critical value; at lithospheric temperatures, however, this critical stress is so large that essentially any realistic lithospheric stress will suffice to generate three solutions. These three solutions represent a cold viscous state (associated with "stick" behavior); an intermediate-temperature (cool) state (associated with "slip" behavior); and lastly a hot low-viscosity state involving strength recovery (i.e., stress once again increases with increasing strain-rate, albeit more gradually given the

low viscosity). Both the cold/high-viscosity and hot/low-viscosity states are stable, while the intermediate-temperature "slip" state is unstable. Thus any initial state wherin there are temperatures both above and below the intermediate-temperature state will evolve toward both the cold and hot states and thus lead to inhomogeneous viscosities and strain-rates, and hence shear-localization. Since the system will evolve to one or more steady states, there is no runaway instability leading to intense or nearly singular plate-boundary-like localization. However, the hot/fast state typically has temperatures well in excess of the melting temperatures of silicates and thus the subsolidus creeping flow model we have used to analyze the thermal feedback mechanism is not valid at these temperatures; with melting, however, shear-localization is due to be more pronounced.

The idealized damage feedback mechanism is mathematically perhaps the simplest of all the feedbacks we considered here. In the case where loss is of decay-type, there are two possible steady deformation states if stress is less than a maximum that is given by a single dimensionless stress $\tau_{max} = 1/2$ (which we estimate to be dimensionally of the order 100 MPa). One of these states correlates to a low-porosity/slow-deformation (stick) state, and the other to a high-porosity/fast-deformation (slip) state. The low-porosity state is stable, while the high-porosity one is unstable. An initial configuration in which there are porosities both above and below the high-porosity state will lead to the porosities below decaying to the low-porosity state, and porosities above undergoing a runaway toward the maximum allowable porosity of 1. This suggests that with this simple feedback mechanism a localization will involve a high porosity band that grows toward a completely voided opening or macrocrack. In the case where the applied stress is greater than τ_{max} then the entire system will undergo a runaway toward a porosity of 1; i.e., the entire layer becomes a highly damaged zone.

Lastly, in the grainsize feedback mechanism there are also two possible deformation states as long as the grainssize dependence of viscosity is nonlinear (i.e., the parameter $m > 1$). However, in contrast to the other two feedback mechanisms, these multiple states only exist if the imposed stress is larger than a minimum value, which itself depends on several other parameters of the mathematical model but is dimensionally of the order 100 MPa or less. These two states involve small-grainsize/fast-deformation and a large-grainsize/slow-deformation states, respectively. Unlike the other feedback mechanisms, the fast-deformation state is stable and the slow one unstable. Thus any configuration that starts off in the vicinity of the slow-deformation state will develop stable localized regions at the fast-deformation state surrounded by slow-deformation regions that become increasingly slower and larger in grainsize. If stress is less than the critical value to obtain multiple states, then the entire system is undergoes grain-growth and progressive stiffening.

The three feedback mechanisms display similarities in that they allow coexisting multiple deformation states. However they differ significantly in other aspects. In particular, for the thermal and damage feedback cases, multiple states and thus shear-localization occurs for stresses beneath a critical value. Above that critical stress, the thermal feedback only allows a cold-viscous state, while the damage feedback allows no steady state and undergoes a runaway to a totally damaged zone. Below the critical stress, the coexisting states become more disparate as stress decreases, thus leading to more pronounced heterogeneity in strain-rate, and thus greater intensity of localization. For the grainsize effect, multiple states are allowed for stress above a critical value; for smaller stresses no steady state is allowed and the system evolves to an ever stiffer and larger-grainsized configuration, while

for higher stresses localization becomes more intense. Therefore, both the thermal and damage feedbacks are in effect low stresses phenomena, while the grainsize feedback is a high-stress phenomenon.

In contrast to the decay-type loss mechanism, a diffusive-type healing mechanism leads to governing equations that depend explicitly on y; the solutions to the equations thus prescribe structure in y and thus permit self-focussing and localization without arbitrary dependence on initial conditions. As with the decay-type loss, multiple solutions and thus deformation states are allowed for a given imposed stress; however, these states do not co-exist in the deforming layer since each state is prescribed by the governing equations to exist over the entire width of the layer. For the thermal feedback mechanism, there are three possible states wherein the coldest and hottest have more or less uniform viscosity and very weak localization, and an intermediate state that involves moderate localization. The existence of these states also depends on the background or boundary temperature; if this temperature is too high then there is no intermediate localizing state, and thus in this case it is clear that localization is a lower-temperature phenomenon (although the background temperature that permits localization is typical of lithospheric temperature of the order 1000 K). For the damage feedback mechanism, there are two possible states: a low-porosity/slow-deformation state with little or no shear localization, and one with a high-porosity and rapidly deforming zone and thus very intense shear localization. Again with both cases, localization only occurs beneath a maximum stress, and the smaller the imposed stress the more intense the localization for the fast solutions, and the more uniform the strain-rate for the slow solutions. Lastly, it appears that the damage feedback mechanism permits much more intense localization than the thermal feedback, which also corresponds to the two-dimensional calculations discussed briefly above.

The diffusive loss for the grainsize mechanism was not studied since it is unlikely to be relavant for that mechanism. Moreover, the stability of cases with diffusive loss was not studied here because it is not analytically tractable, and it would require many numerical solutions to properly examine. However, the diffusive loss mechanism is likely to stabilize states whose analogs in the decay-loss mechanism cases were unstable; this is because the sharpening of a thermal anomaly during localization enhances diffusive loss while having no effect in the decay-loss scenario. However, diffusion does not completely stabilize these cases since it is known to still permit thermal instabilities and runaways to large-strain-rate solutions (Yuen and Schubert 1977; Schubert and Yuen 1978; Fleitout and Froidevaux 1980). Nevertheless, it should be noted that instabilities and runaway effects can be supressed if we impose a constant velocity across the shear layer, instead of a constant stress. This is because shear-localization instability and runaway involve changes in boundary velocities as well as strain-rates (e.g., Eqn. 71 to Eqn. 72 suggest that the boundary velocity and the sharpness of the shear-localization zone both increase as localization intensifies); however, if the boundary velocity is fixed then such instability is simply prohibited.

Finally, we should note that since the thermal feedback mechanism does not permit a runaway instability (at least not without melting) it is perhaps the weakest of the localization mechanisms (this is also evident in the structure of the steady-state solutions with diffusive loss, at least relative to the damage feedback mechanism; i.e. compare the localized solutions for Figs. **4** and **5**). In contrast, the damage and grainsize feedback mechanisms do allow runaway effects and/or intense localization and thus are perhaps the more likely candidates to generate plate-boundary-like localizations in the lithosphere. The physics

of these processes, however, are still not completely well understood and considerable research remains to elucidate their nature. However, it is also important to note the possible relation between the grainsize and damage mechanisms: both involve creation of surface energy, through the creation of more grain boundaries by propagating dislocations in one, and the creation of fracture surfaces through microcracking in the other, which are more or less manifestations of the same physics. In the end, shear-localization in a geological and geophysical context is a difficult but rich topic with considerable room for further progress and discovery from theoretical, experimental and observational aspects.

REFERENCES

Ashby M, Sammis C (1990) The damage mechanics of brittle solids in compression. Pure Appl Geophys 133:489–521

Atkinson B (1987) Introduction to fracture mechanics and its geophysical applications. *In* Atkinson B (ed) Fracture Mechanics of Rock. Academic, San Diego, CA, 1–26

Atkinson B, Meredith P (1987) Experimental fracture mechanics data for rocks and minerals. *In* Atkinson B (ed) Fracture Mechanics of Rock. Academic, San Diego, CA, 427–525

Auth C, Bercovici D, Christensen U (2002) Two-dimensional convection with a self-lubricating, simple-damage rheology. Geophys J Int (in press)

Balachandar S, Yuen D, Reuteler D (1995) Localization of toroidal motion and shear heating in 3-D high Rayleigh number convection with temperature-dependent viscosity. Geophys Res Lett 22:477–480

Beaumont C (1976) The evolution of sedimentary basins on a viscoelastic lithosphere. Geophys J R Astron Soc 55:471–497

Bercovici D (1993) A simple model of plate generation from mantle flow. Geophys J Int 114:635–650

Bercovici D (1995a) On the purpose of toroidal flow in a convecting mantle. Geophys Res Lett 22:3107–3110

Bercovici D (1995b) A source-sink model of the generation of plate tectonics from non-Newtonian mantle flow. J Geophys Res 100:2013–2030

Bercovici D (1996) Plate generation in a simple model of lithosphere-mantle flow with dynamic self-lubrication. Earth Planet Sci Lett 144:41–51

Bercovici D (1998) Generation of plate tectonics from lithosphere-mantle flow and void-volatile self-lubrication. Earth Planet Sci Lett 154:139–151

Bercovici D (2003) The Generation of plate tectonics from mantle convection. Earth Planet Sci Lett 205:107–121

Bercovici D, Ricard Y (2003) Energetics of a two-phase model of lithospheric damage, shear localization and plate-boundary formation. Geophys J Intl 152:1–16

Bercovici D, Ricard Y, Richards M (2000) The relation between mantle dynamics and plate tectonics: A primer. *In* Richards MA, Gordon R, van der Hilst R (eds) History and Dynamics of Global Plate Motions, Geophys Monogr Ser 121:5–46

Bercovici D, Ricard Y, Schubert G (2001a) A two-phase model of compaction and damage, 1. General theory. J Geophys Res 106:8887–8906

Bercovici D, Ricard Y, Schubert G (2001b) A two-phase model of compaction and damage, 3. Applications to shear localization and plate boundary formation. J Geophys Res 106:8925–8940

Braun J, Chery J, Poliakov A, Mainprice D, Vauchez A, Tomassi A, Daignieres M (1999) A simple parameterization of strain localization in the ductile regime due to grain size reduction: A case study for olivine. J Geophys Res 104:25,167–25,181

Bresser JD, Peach C, Reijs J, Spiers C (1998) On dynamic recrystallization during solid state flow: Effects of stress and temperature. Geophys Res Lett 25:3457–3460

Bresser JD, ter Heege J, Spiers C (2001) Grain size reduction by dynamic recrystallization: can it result in major rheological weakening? Intl J Earth Sci 90:28–45

Cooper R, Kohlstedt D (1982) Interfacial energies in the olivine-basalt system. *In* Akimoto S, Manghnani M (eds) High Pressure Research in Geophysics, Adv Earth Planet Sci 12:217–228

Cottrell A (1953) Dislocations and Plastic Flow in Crystals. Clarendon Press, Oxford, UK

Derby B, Ashby M (1987) On dynamic recrystallization. Scripta Metall 21:879–884

Evans B, Kohlstedt D (1995) Rheology of rocks. *In* Ahrens TJ (ed) Rock Physics and Phase Relations: A Handbook of Physical Constants. AGU Ref Shelf, vol 3. Am Geophys Union, Washington, DC, 148–165

Farren W, Taylor G (1925) The heat developed during plastic extension of metals. Proc R Soc London Ser A 107:422–451

Fleitout L, Froidevaux C (1980) Thermal and mechanical evolution of shear zones. J Struct Geol 2:159–164

Frederiksen S, Braun J (2001) Numerical modelling of strain localisation during extension of the continental lithosphere. Earth Planet Sci Lett 188:241–251

Frost H, Ashby M (1982) Deformation Mechanism Maps. Pergamon Press, Oxford, UK

Furusho M, Kanagawa K (1999) Reaction induced strain localization in a lherzolite mylonite from the Hidaka metamorphic belt of central Hokkaido, Japan. Tectonophysics 313:411–432
Géminard JC, Losert W, Gollub J (1999) Frictional mechanics of wet granular material. Phys Rev E 59:5881–5890
Green H, Burnley P (1989) A new self-organizing mechanism for deep focus earthquakes. Nature 341:733–737
Griffith A (1921) The phenomenon of rupture and flow in solids. Philos Trans R Soc London, Ser A 221:163–198
Guéguen Y, Palciauskas V (1994) Introduction to the Physics of Rocks. Princeton University Press, Princeton, New Jersey
Gurnis M, Zhong S, Toth J (2000) On the competing roles of fault reactivation and brittle failure in generating plate tectonics from mantle convection. *In* Richards M, Gordon R, van der Hilst R (eds) History and Dynamics of Global Plate Motions, Geophys Monogr Ser 121:73–94
Handy M (1994) Flow laws for rocks containing two nonlinear viscous phases: a phenomenological approach. J Struct Geol 16:287–301
Hansen N, Schreyer H (1992) Thermodynamically consistent theories for elastoplasticity coupled with damage. *In* Ju J, Valanis K (eds) Damage Mechanics and Localization. Am Soc Mech Eng, New York, 53–67
Hirth G, Kohlstedt D (1996) Water in the oceanic upper mantle: implications for rheology, melt extraction and the evolution of the lithosphere. Earth Planet Sci Lett 144:93–108
Jaeger J, Cook N (1979) Fundamentals of Rock Mechanics. 3rd edn. Chapman and Hall, New York
Jin D, Karato S, Obata M (1998) Mechanisms of shear localization in the continental lithosphere: Inference from the deformation microstructures of peridotites from the Ivrea zone, northwestern Italy. J Struct Geol 20:195–209
Kameyama M, Yuen D, Fujimoto H (1997) The interaction of viscous heating with grain-size dependent rheology in the formation of localized slip zones. Geophys Res Lett 24:2523–2526
Karato S (1996) Plastic flow in rocks. *In* Matsui T (ed) Continuum Physics, Earth and Planetary Sciences Series, vol 6. Iwani Shoten, Tokyo, 239–291
Karato S (2002) Mapping water content in the upper mantle. *In* Eiler J, Abers J (eds) Subduction Factory, Monograph, Am Geophys Union, Washington, DC, (in press)
Karato S, Riedel M, Yuen D (2001) Rheological structure and deformation of subducted slabs in the mantle transition zone: implications for mantle circulation and deep earthquakes. Phys Earth Planet Int 127:83–108
Karato S, Toriumi M, Fujii T (1980) Dynamic recrystallization of olivine single crystals during high temperature creep. Geophys Res Lett 7:649–652
Kirby S (1987) Localized polymorphic phase transformations in high-pressure faults and applications to the physical mechanisms of deep earthquakes. J Geophys Res 92:13,789–13,800
Kohlstedt D, Evans B, Mackwell S (1995) Strength of the lithosphere: Constraints imposed by laboratory experiments. J Geophys Res 100:17,587–17,602
Krajcinovic D (1996) Damage Mechanics. North-Holland, Amsterdam
Krajcinovic D (2000) Damage mechanics: accomplishments, trends and needs. Intl J Solids Struct 37:267–277
Lee K, Jiang Z, Karato S (2002) A scanning electron microscope study of effects of dynamic recrystallization on the lattice preferred orientation in olivine. Tectonophysics 351:331–341
Lemaitre J (1992) A Course on Damage Mechanics. Springer-Verlag, New York
Lemonds J, Needleman A (1986) Finite element analyses of shear localization in rate and temperature dependent solids. Mech Mater 5:339–361
Lockner D (1995) Rock failure. *In* Ahrens TJ (ed) Rock Physics and Phase Relations: A Handbook of Physical Constants, AGU Ref Shelf, vol. 3. Am Geophys Union, Washington, DC, 127–147
Lyakhovsky V, Ben-Zion Y, Agnon A (1997) Distributed damage, faulting, and friction. J Geophys Res 102:27,635–27,649
Marone C (1998) Laboratory-derived friction laws and their application to seismic faulting. Ann Rev Earth Planet Sci 26:643–696
Mathur K, Needleman A, Tvergaard V (1996) Three dimensional analysis of dynamic ductile crack growth in a thin plate. J Mech Phys Solids 44:439–464
Montési L, Zuber M (2002) A unified description of localization for application to largescale tectonics. J Geophys Res 107:10.1029/2001JB000465
Mora P, Place D (1998) Numerical simulation of earthquake faults with gouge: Toward a comprehensive explanation for the heat flow paradox. J Geophys Res 103:21,067–21,089
Ogawa M (2002) The plate-like regime of a numerically modeled thermal convection in a fluid with temperature-, pressure-, and stress-history-dependent viscosity. J Geophys Res (in press)
Paterson M (1978) Experimental Rock Deformation. Springer-Verlag, Berlin
Poirier J (1980) Shear localization and shear instability in materials in the ductile field. J Struct Geol 2:135–142
Poirier J (1985) Creep of Crystals. Cambridge University Press, Cambridge, UK

Ranalli G (1995) Rheology of the Earth. Chapman and Hall Publishers, London
Regenauer-Lieb K (1999) Dilatant plasticity applied to Alpine collision: Ductile void-growth in the intraplate area beneath the Eifel volcanic field. J Geodyn 27:1–21
Regenauer-Lieb K, Yuen D (2002) Modeling shear zones in geological and planetary sciences: solid- and fluid- thermal-mechanical approaches. Earth Sci Rev (in press)
Ricard Y, Bercovici D (2002) The void-matrix variation of a two-phase damage theory; applications to shear localization and shear-enhanced compaction. Geophys J Intl (submitted)
Ricard Y, Bercovici D, Schubert G (2001) A two-phase model of compaction and damage, 2, Applications to compaction, deformation, and the role of interfacial surface tension. J Geophys, Res 106:8907–8924
Riedel M, Karato S (1997) Grain-size evolution in subducted oceanic lithosphere associated with the olivine-spinel transformation and its effects on rheology. Earth Planet Sci Lett 148:27–43
Rubie D (1983) Reaction-enhanced ductility: The role of solid-solid univariant reactions in deformation of the crust and mantle. Tectonophysics 96:331–352
Rubie D (1984) The olivine-spinel transformation and the rheology of subducting lithosphere. Nature 308:505–508
Schubert G, Turcotte D (1972) One-dimensional model of shallow mantle convection. J Geophys Res 77:945–951
Schubert G, Yuen D (1978) Shear heating instability in Earth's upper mantle. Tectonophysics 50:197–205
Scott D (1996) Seismicity and stress rotation in a granular model of the brittle crust. Nature 381:592–595
Segall P, Rice JR (1995) Dilatancy, compaction, and slip instability of a fluid-infiltrated fault. J Geophys Res 100:22,155–22,171
Shimizu I (1998) Stress and temperature dependence of recrystallized grain size: A subgrain misorientation model. Geophys Res Lett 25:4237–4240
Sleep N (1995) Ductile creep, compaction, and rate and state dependent friction within major faults. J Geophys Res 100:13,065–13,080
Sleep N (1997) Application of a unified rate and state friction theory to the mechanics of fault zones with strain localization. J Geophys Res 102:2875–2895
Stünitz H, Tullis J (2001) Weakening and strain localization produced by syndeformational reaction of plagioclase. Intl J Earth Sci 90:136–148
Tackley P (1998) Self-consistent generation of tectonic plates in three-dimensional mantle convection. Earth Planet Sci Lett 157:9–22
Tackley P (2000a) Mantle convection and plate tectonics: Toward and integrated physical and chemical theory. Science 288:2002–2007
Tackley P (2000b) The quest for self-consistent generation of plate tectonics in mantle convection models. *In* Richards MA, Gordon R, van der Hilst R (eds) History and Dynamics of Global Plate Motions, Geophys Monogr Ser 121:47–72
Tackley P (2000c) Self-consistent generation of tectonic plates in time-dependent, three-dimensional mantle convection simulations, 1. Pseudoplastic yielding. Geochem Geophys Geosystems (G^3) 1:2000GC000,036
Tackley P (2000d) Self-consistent generation of tectonic plates in time-dependent, three-dimensional mantle convection simulations, 2. Strain weakening and asthenosphere. Geochem Geophys Geosystems (G^3) 1:2000GC000,043
Taylor G, Quinney H (1934) The latent energy remaining in metal after cold working. Proc R Soc London, Ser A 143:307–326
Thatcher W, England P (1998) Ductile shear zones beneath strike-slip faults: Implications for the thermomechanics of the San Andreas fault zone. J Geophys Res 103:891–905
Tozer D (1985) Heat transfer and planetary evolution. Geophys Surv 7:213–246
Trompert R, Hansen U (1998) Mantle convection simulations with rheologies that generate plate-like behavior. Nature 395:686–689
Turcotte D, Schubert G (1982) Geodynamics. John Wiley & Sons, New York
Urai J, Means W, Lister G (1986) Dynamic recrystallization in minerals. *In* Hobbs B, Heard H (eds) Mineral and Rock Deformation: Laboratory Studies. American Geophysical Union, Washington DC, 166–199
Watts A, Karner G, Steckler M (1982) Lithosphere flexure and the evolution of sedimentary basins. Philos Trans R Soc London, Ser A 305:249–281
White S, Burrows S, Carreras J, Shaw N, Humphreys F (1980) On mylonites in ductile shear zones. J Struc. Geol. 2:175–187
Whitehead J, Gans R (1974) A new, theoretically tractable earthquake model. Geophys J R Astron Soc 39:11–28
Yuen D, Schubert G (1977) Asthenospheric shear flow: thermally stable or unstable? Geophys Res Lett 4:503–506
Yuen D, Schubert G (1979) The role of shear heating in the dynamics of large ice masses. J Glaciol 24:195–212

13 Theoretical Analysis of Shear Localization in the Lithosphere

David Bercovici and Shun-ichiro Karato